I.

Different interferon-producing capacities of L929 cell sublines and the enhancement of interferon production by priming are controlled pretranslationally

I. Rosztóczy, M. Papós and K. Megyeri

Institute of Microbiology, University Medical School, Szeged Dóm tér 10., H-6720, Hungary

Received 15 September 1986

Two sublines of mouse L929 cells designated L929B and L929M were studied. The L929B cells, which displayed a 2–3-fold higher IFN production in response to Sendai virus than that of the L929M cells, had a higher sensitivity to the antiviral and priming effects of IFN and were more resistant to VSV. In good accord with the amount of IFN produced, more translatable IFN mRNA was isolated from the L929B cells. IFN production and IFN mRNA activities were proportionally increased in the IFN-primed cultures of both sublines. Results indicate that both inherent and priming-induced increased-IFN production are based on pretranslational control mechanisms.

Interferon production *Pretranslational control* *Priming effect*

1. INTRODUCTION

A wide variation of control mechanisms exists for the regulation of expressions of inducible proteins in eukaryotic cells. IFNs are proteins with antiviral, cell growth-inhibitory and immunomodulatory activities, synthesized by cells upon virus infection or treatment with double-stranded nucleic acids. The effectivity of IFN induction is dependent on the type of the producing cell and on the nature of the inducer. It has also been reported that the treatment of cells with homologous IFN before induction primes subsequent IFN production [1]. The point of attack of priming in the process of IFN synthesis has been extensively studied, but there is some disagreement as to the exact nature of the process involved [2–5]. Since we have isolated two L929 sublines that had different IFN-producing capacities and in which there were different degrees of enhancement of IFN production by priming, we considered them as advantageous tools which might provide comprehensive data on the mechanisms determining the effectivities of IFN production and of priming. The main objective of the present work was therefore to determine whether the enhanced IFN production under these conditions was also manifested in the amount of IFN mRNA or not. In order to answer this question, we compared the titres of IFN produced and the amounts of translatable IFN mRNA in these two sublines of L929 cells.

Abbreviations: FCS, fetal calf serum; HAU, hemagglutinating unit; IFN, interferon; IU, international unit; MEM, minimal Eagle's medium; PFU, plaque forming unit; $TCID_{50}$, tissue culture infectious dose 50; VSV, vesicular stomatitis virus

2. MATERIALS AND METHODS

2.1. *Cells*

The sublines L929B and L929M were isolated after serial mutagenesis from a mouse L929 cell line originally provided by G.L. Toms (Department of Microbiology, University of Birmingham,

Published by Elsevier Science Publishers B.V. (Biomedical Division)
00145793/86/$3.50

Birmingham, England). Both sublines were serially passaged in MEM supplemented with 5% FCS and antibiotics. Their characteristics were not reversed during more than 50 passages of the cells.

2.2. *IFN titration*

This was carried out as described [6]. IFN titres are given in reference units.

2.3. *Extraction and assay of IFN mRNA*

The poly(A)-containing RNA fraction was isolated from the IFN-producing cells with the method of Ullrich et al. [7]. The translational activity of IFN mRNA present in these preparations was quantitated by injection into *Xenopus laevis* oocytes [8]. The titre of translated IFN was determined on mouse L929 cells.

Table 1

Characteristics of L929B and L929M sublines and the IFNs they produce

Characteristics	Cells	
	L929B	L929M
Population doubling time (h)	21	21
Spontaneous IFN formation	none	none
50% virus inhibitory concentration of IFN (IU/ml)	0.15	0.8
Minimal priming dose of IFN (IU/ml)	0.1	1.0
$TCID_{50}$ of VSV (PFU/ml)[a]	6.8×10^4	7.0×10^1
Neutralization titre of MuIFN antiserum against the IFN produced[b]	2.4×10^4	2.4×10^4
Residual activity of IFN after 30 min at 56°C (%)	1.5–2	1.5–2
Molecular masses of peak IFN activities (kDa)[c]	22–24 28–32	22–24 28–32

[a] The VSV preparation used for determination of the susceptibilities of L929 cells to this virus had a titre of $10^{7.9}$ PFU/ml on primary chick embryo fibroblasts

[b] Dilution of MuIFN antiserum (G-024-501-568; provided by the Antiviral Substances Program, National Institute of Health, Bethesda, MD, USA) required for neutralization of 10 IU of IFN produced by L929B or L929M cells

[c] Gel filtration analysis of IFNs was performed on a Sephadex G-75 column (2.5 × 70 cm)

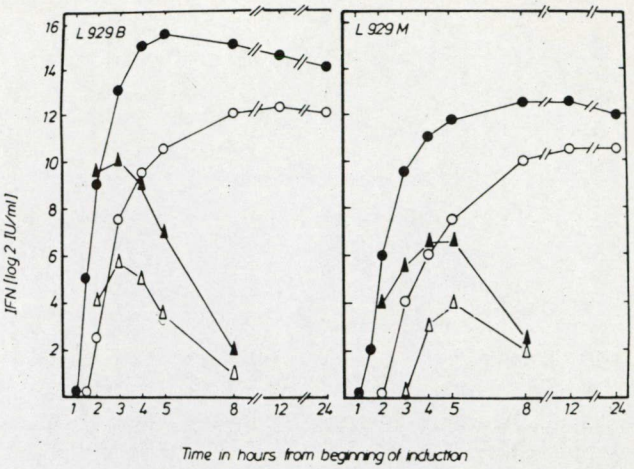

Fig.1. Effects of IFN pretreatment on IFN production and IFN mRNA content of L929B and L929M cells. Confluent cultures grown in 150 cm^2 plastic tissue culture flasks were pretreated for 10 h with 30 IU/ml of a partially purified preparation of mouse L cell IFN with a specific activity of $10^{6.5}$ IU/mg protein. For IFN induction 3 ml of 1.8×10^3 HAU/ml concentrated and purified Sendai virus (parainfluenza 1) was added to each flask, after which 1×10^8 cells were collected at different times for the determination of IFN mRNA content. The IFN production was determined on the corresponding culture media. (○) Control IFN; (●) primed IFN; (△) control IFN mRNA; (▲) primed IFN mRNA. The points represent mean values of four independent experiments.

3. RESULTS

The L929B subline was about 5–10-times more susceptible to the antiviral and priming effects of IFN, and approx. 1000-times more VSV was required to infect these cells than L929M cells. However, we found no difference between the immunological and physico-chemical characteristics of the IFNs produced by them (table 1).

Unprimed (control) L929B cells produced 2–3-times more IFN than did L929M cells. For the primed cultures the corresponding ratio was approx. 2-times higher and the kinetics of IFN production was accelerated. The amount of translatable IFN mRNA was proportional to the amount of IFN produced. The L929B cells, which produced more IFN in response to induction with Sendai virus, likewise contained more IFN mRNA than did the L929M cells. The enhancement of IFN production and the amount of IFN mRNA were also proportional in response to priming (fig.1).

4. DISCUSSION

The higher IFN mRNA levels in L929B cells indicate that the inherent differences in IFN-producing capacities are manifested pretranslationally.

Our results permit localization of the point of attack of priming at a pretranslational level. This supports the findings of Sehgal and Gupta [9] and Fujita and Kohno [10], but is at variance with the results of Abreu et al. [3] and Content et al. [5], who suggested that priming affects IFN production at the level of translation too. The proportional enhancement of the amount of IFN mRNA to that of IFN production in the primed L929B and L929M cells, together with the exclusion of a longer half-life of HuIFN-beta mRNA [11] and the enhanced rate of transcription of the HuIFN-beta gene [12] in primed human fibroblast, seem to indicate that the transcription of IFN messages is the primary target of priming.

REFERENCES

[1] Isaacs, A. and Burke, D.C. (1958) Nature 182, 1073–1074.
[2] Lebleu, B., Hubert, E., Content, J., De Wit, L., Braude, I.A. and De Clercq, E. (1978) Biochem. Biophys. Res. Commun. 82, 665–673.
[3] Abreu, S.L., Bancroft, F.C. and Stewart, W.E. ii (1979) J. Biol. Chem. 254, 4114–4118.
[4] Fujita, T., Saito, S. and Kohno, S. (1979) J. Gen. Virol. 45, 301–308.
[5] Content, J., Johnston, M.I., De Wit, L., De Maeyer-Guignard, J. and De Clercq, E. (1980) Biochem. Biophys. Res. Commun. 96, 415–424.
[6] Rosztóczy, I. (1976) Acta Virol. 20, 472–478.
[7] Ullrich, A., Shine, J., Chirgwin, J., Pictet, R., Tischer, E., Rutter, W.J. and Goodman, H.M. (1977) Science 196, 1313–1319.
[8] Rosztóczy, I. and Siroki, O. (1985) Acta Microbiol. Hung. 32, 351–356.
[9] Sehgal, P.B. and Gupta, S.L. (1980) Proc. Natl. Acad. Sci. USA 77, 3489–3493.
[10] Fujita, T. and Kohno, S. (1981) Virology 112, 62–69.
[11] Raj, N.B.K. and Pitha, P.M. (1981) Proc. Natl. Acad. Sci. USA 78, 7426–7430.
[12] Nir, U., Maroteaux, L., Cohen, B. and Mory, I. (1985) J. Biol. Chem. 260, 14242–14247.

II.

JOURNAL OF INTERFERON RESEARCH 12:13–16 (1992)
Mary Ann Liebert, Inc., Publishers

Interferon Pretreatment Regulates Interferon and Interleukin-6 Production in L929 Cells in a Coordinated Manner

I. ROSZTOCZY,[1] J. CONTENT,[2] and K. MEGYERI[1]

ABSTRACT

Two sublines of L929 cells with different interferon (IFN)-producing capacities synthesized IFN and interleukin-6 (IL-6) simultaneously in response to Sendai virus infection. IFN pretreatment primed the production of both cytokines. However, the difference in IL-6 production between the "high and low producer" L-cell sublines was about one magnitude of order larger than in the case of their IFN production. The determination of the corresponding mRNA levels also reflected this difference.

PRETREATMENT OF CELLS with homologous interferon (IFN) can enhance their subsequent IFN production induced either by viruses or by dsRNA.[1,2] Besides this priming effect on its own production, IFN can modulate the production of some other cytokines, such as interleukin-1 (IL-1), IL-2, and tumor necrosis factor (TNF).[3–6] Kohase *et al.* reported the enhancing effect of IFN-β on TNF-induced IL-6 expression.[7] IL-6 was observed to be synthesized simultaneously with IFN-β in human embryo fibroblasts.[3,8] We recently isolated two L929 cell sublines with different IFN-producing capacities in response to Sendai virus.[9] Sendai virus has been shown to induce IL-6 production in cultures of human fibroblasts and mouse L929 cells.[10,11] Our observation indicated that priming enhances differently the Sendai virus-induced IFN production in L-cell sublines with different susceptibilities to the antiviral effect of IFN.[9] Since our previous study showed that the synthesis of IFN-β was extensively modulated by priming, it was of interest to see how the expression of IL-6 is affected when simultaneous IFN production is primed with IFN pretreatment.

MATERIALS AND METHODS

Cells: The two sublines of mouse L929 cells, designated LB and LM, and their culture conditions were the same as described previously.[9]

IFN and IL-6 Assays: IFN was assayed as described earlier[12]; the titers are given in international reference units (IU/ml). IL-6 activity was determined by utilizing the IL-6–dependent mouse–mouse hybridoma 7TD1 cells kindly provided by J. Van Snick (Ludwig Institute for Cancer Research, Brussels, Belgium). The assay procedure was the same as described by the above author.[13] The titrations were carried out using the human IL-6 WHO standard preparations, and the results are given in reference units. For titering the oocyte supernatants, dilutions started from 1:6, as the higher concentrations decreased the viability of the 7TD1 cells.

IFN and IL-6 activities in culture media of the L929 sublines were characterized with antiserum to murine (Mu) IFN-β (Lee Biomolecular Research Lab, Inc.) and rat anti-mouse IL-6 monoclonal antibody (Genzyme Corp.). The cytokine preparations were diluted to about 200 IU/ml concentration and the antisera were added in equal volume that contained twofold excess of neutralizing potency relative to the cytokines biological activity.

Extraction and Assay of IFN and IL-6 mRNAs: Polyadenylated RNA was prepared from the differently treated cultures of L-cell sublines with a modification of the method of Cox and Smulian.[14] For biological assay, 30-nl portions of 1 mg/ml poly(A)$^+$ RNA solutions were injected into each oocyte. Fifteen oocytes were injected with one preparation and were incubated in 150 μl of Barth medium for 36 h at 22°C. The supernatant was then assayed for IFN and IL-6 activities as described above. Total RNA was isolated by guanidine thiocyanate method and the levels of IL-6 mRNA were monitored by agarose gel electrophoresis followed by blot hybridization using a murine IL-6 riboprobe. The probe was synthesized from a 650-bp *Eco* RI–*Bgl* II fragment of murine IL-6 cDNA cloned into pSP64.

[1]Institute of Microbiology, Albert Szent-Gyorgyi Medical University, Szeged, Hungary; [2]Institut Pasteur du Brabant, Brussels, Belgium.
Received 8 August 1990/accepted 13 September 1991

RESULTS

IFN and IL-6 production by LB and LM cells in response to Sendai virus

IFN and IL-6 assays of 20-h culture media from the Sendai virus stimulated L929 cell sublines indicated the simultaneous presence of both IFN and IL-6 activities. Cytokines were serologically characterized by neutralization with appropriate antisera. The treatment of samples with antiserum to MuIFN-β neutralized the IFN activity but did not affect the IL-6 activity or vice versa (Table 1).

Effect of IFN pretreatment on IFN and IL-6 production and their mRNA levels

The release of IFN and IL-6 activities from both L929 cell sublines after Sendai virus induction followed a fairly similar pattern. The IL-6 activity from the "high-producer" subline (LB) always exceeded the amount of IFN present when expressed in IU/ml. In contrast, the LM-cells ("low-producer") synthesized less IL-6 than IFN. Pretreatment of cultures with MuIFN-α/β enhanced the production of both cytokines. However, the level of enhancement was more pronounced in the LB cell subline (Fig. 1). It can be seen from the data presented in Table 2 that the injection of poly(A) plus RNA into *Xenopus laevis* oocytes resulted in the translation of quasi-proportional amounts of IFN and IL-6 activities with respect to those detected in culture supernatants. In the case of IL-6, this observation was also confirmed with blot hybridization analysis (Fig. 2). Determination of the antigenicities of the primed and unprimed IFN samples and the oocyte-translated products indicated the abundance of MuIFN-β because the biological activity was resistant to pH 2 treatment and ≥90% was neutralized with the MuIFN-β antiserum. Similar to the IL-6 activity found in the culture media of L929 cells, the oocyte-translated IL-6 activity was also neutralized by the rat anti-mouse IL-6 antibody (data not shown).

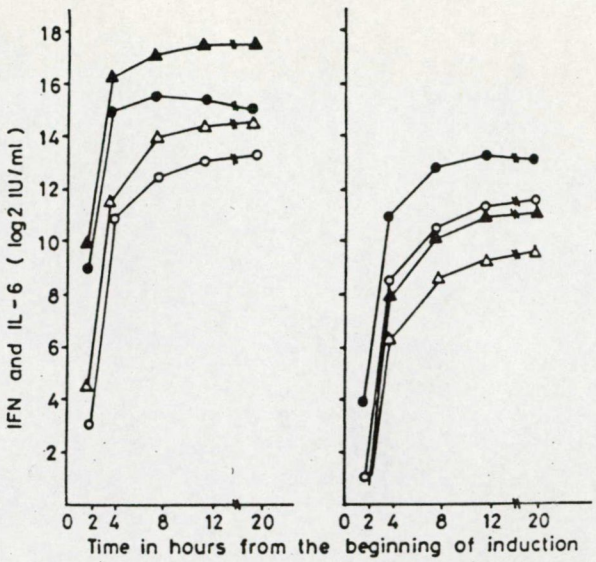

Fig. 1. Effects of MuIFN-α/β pretreatment on IFN and IL-6 production by LB and LM cells. L cells were pretreated for 8 h with 30 IU/ml of MuIFN-α/β (sp. act., 1.2×10^8 IU/mg protein). For the induction of cells, 10 ml of 2×10^2 hemagglutinating units (HAU)/ml concentrated and purified Sendai virus (parainfluenza virus 1) was added in Dulbecco's minimal essential medium (DMEM) without fetal calf serum (FCS) to each 150-cm^2 flask. After incubation for 1 h at 37°C in 5% CO_2 in air, the virus was replaced with 20 ml of prewarmed medium supplemented with 5% FCS. Cells and culture media were collected at different times for the determination of IFN and IL-6 activities and for extraction of poly(A)$^+$ RNA. Left panel, LB cells. Right panel, LM cells. *y* axis, IFN and IL-6 (log 2 IU/ml); *x* axis, time in hours from the beginning of induction. Designations used are: IFN in control (○) and in primed (●) cultures; IL-6 in control (△) and in primed (▲) cultures.

DISCUSSION

There are several cytokines whose synthesis can be detected simultaneously under certain conditions.[15–18] Our results confirm the observation reported by Kohase *et al.*[7] showing the enhancing effect of IFN on IL-6 production. In addition, we observed that pretreatment of cells with homologous IFN primed both IFN and IL-6 production when these cytokines were synthesized simultaneously. This suggests that, in spite of the different chromosomal localization of MuIFN-β and IL-6 genes,[19,20] their expression seems to be coordinately regulated upon both inductive and IFN-evoked modulatory signals. The coordinated up-regulation to priming may be based on positive *cis* regulatory elements in the 5′-flanking region of MuIFN-β and IL-6 genes[21–23] interacting with the same IFN-induced transacting factors. The NF-κB is a candidate of this function because its binding site is the only known common element between the two promoters.[23,24]

TABLE 1. SEROLOGIC CHARACTERIZATION OF SIMULTANEOUSLY PRODUCED IFN AND IL-6 ACTIVITIES

Cytokine	*Producing cells*	*Residual activity (IU/ml) after treatment*		
		Medium	*Anti IFN-β*	*Anti IL-6*
IFN	LB	110	<4	76
	LM	96	<4	90
IL-6	LB	80	70	<4
	LM	72	64	<4

Data represent the mean values of two independent determinations.

ACKNOWLEDGMENTS

The critical reading of the manuscript by N.B.K. Raj is gratefully acknowledged. We also thank Zsuzsanna Czapff and Barbara Schneider for their help in the preparation of the manuscript.

TABLE 2. *IN VITRO* TRANSLATION OF IFN AND IL-6 mRNA ACTIVITIES FROM PRIMED AND UNPRIMED LB AND LM CELLS INDUCED BY SENDAI VIRUS

			Activity (IU/ml)	
Cell	*Cytokine*	*Priming*	*2 h*	*4 h*
LB	IFN	+	256	256
		−	18	40
	IL-6	+	1536	1280
		−	48	128
LM	IFN	+	10	24
		−	2	8
	IL-6	+	<6	12
		−	<6	<6

A total of 5×10^7 cells representing one sample were homogenized in 8 ml of 4 *M* guanidine/thiocyanate in 0.1 *M* Tris/HCl, pH 7.5, in a Sorvall omnimixer. Before oligo(dT)-cellulose chromatography, the homogenate was diluted with 8 ml of 1 *M* NaCl/10 mM Tris/HCl, pH 7.5, solution. Following one repeated cycle at room temperature, the oligo(dT)-cellulose column was eluted with 10 m*M* Tris/HCl, pH 7.5. The RNA concentration was measured by optical density at 260 nm. The RNA-containing fractions were pooled and ethanol-precipitated. The precipitate was dissolved in distilled water to give a final concentration of 1 mg/ml and microinjected into *X. laevis* oocytes.

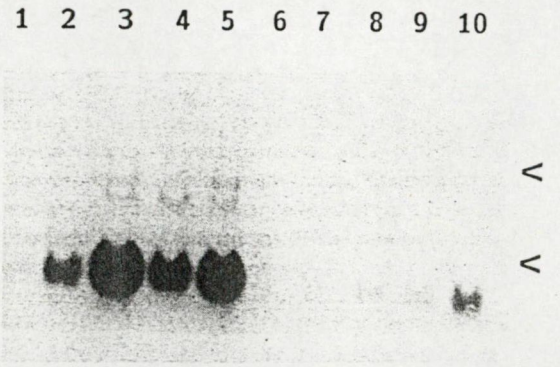

Fig. 2. Time course of IL-6 mRNA appearance in LB and LM cells. RNA extracted from primed and unprimed LB and LM cells was analyzed by blot hybridization with a murine IL-6 riboprobe. Arrowheads indicate the localization of 18S and 28S ribosomal RNAs. Lanes 1–5, LB and 6–10 LM cells. Lanes 1 and 6, untreated control; lanes 2, 3, 7, and 8, 2-h samples; lanes 4, 5, 9, and 10, 4-h samples; lanes 2, 3, 4, 5, 7, 8, 9, and 10, induced with Sendai virus; lanes 3, 5, 8, and 10, primed with IFN pretreatment before induction.

REFERENCES

1. ISAACS, A., and BURKE, D.C. (1958). Mode of action of interferon. Nature **182**, 1073–1074.
2. ROSZTOCZY, I. (1971). Interferon production by polyinosinic-polycytidylic acid in interferon pretreated L cells in absence of DEAE-dextran. Acta Virol. **15**, 431.
3. CONTENT, J., DE WIT, L., PIERARD, D., DERYNCK, R., DE CLERCQ, E., and FIERS, W. (1982). Secretory proteins induced in human fibroblasts under conditions used for the production of interferon-β. Proc. Natl. Acad. Sci. USA **79**, 2768–2772.
4. ROSZTOCZY, I., SIROKI, O., and BELADI, I. (1986). Effects of interferons-α, -β, and -γ on human interleukin-2 production. J. Interferon Res. **6**, 581–589.
5. SAXENA, S., NOURI-ARIA, K.T., ANDERSON, M.G., EDDLESTON, A.L.W., and WILLIAMS, R. (1986). Interleukin 2 activity in chronic liver disease and the effect of *in vitro* α-interferon. Clin. Exp. Immunol. **63**, 541–548.
6. SCUDERI, P., STERLING, K.E., RAITANO, A.B., GROGAN, T.M., and RIPPE, R.A. (1987). Recombinant interferon-γ stimulates the production of human tumor necrosis factor *in vitro*. J. Interferon Res. **7**, 155–164.
7. KOHASE, M., MAY, L.T., TAMM, I., VILČEK, J., and SEHGAL, P.B. (1987). A cytokine network in human diploid fibroblasts: Interactions of β-interferons, tumor necrosis factor, platelet-derived growth factor, and interleukin-1. Mol. Cell. Biol. **7**, 273–280.
8. WEISSENBACH, J., CHERNAJOVSKY, Y., ZEEVI, M., SHULMAN, L., SOREQ, H., NIR, U., WALLACH, D., PERRICAUDET, M., TIOLLAIS, P., and REVEL, M. (1980). Two interferon mRNAs in human fibroblasts: *In vitro* translation and *Escherichia coli* cloning studies. Proc. Natl. Acad. Sci. USA **77**, 7152–7156.
9. ROSZTOCZY, I., PAPOS, M., and MEGYERI, K. (1986). Different interferon-producing capacities of L929 cell sublines and the enhancement of interferon production by priming are controlled pretranslationally. FEBS Lett. **208**, 56–58.
10. SEHGAL, P.B., HELFGOTT, D.C., SANTHANAM, U., TATTER, S.B., CLARICK, R.H., GHRAYER, J., and MAY, L.T. (1988). Regulation of the acute phase and immune responses in viral disease. Enhanced expression of the β_2-interferon/hepatocyte-stimulating factor/interleukin 6 gene in virus-infected human fibroblasts. J. Exp. Med. **167**, 1951–1956.
11. VAN DAMME, J., SCHAAFSMA, M.R., FIBBE, W.E., FALKENBURG, J.H.F., OPDENAKKER, G., and BILLIAU A. (1989). Simultaneous production of interleukin 6, interferon-β and colony-stimulating activity by fibroblasts after viral and bacterial infection. Eur. J. Immunol. **19**, 163–168.
12. ROSZTOCZY, I. (1976). Study of the priming effect of interferon in L cells. I. The primed interferon response and the kinetics of development of priming. Acta Virol. **20**, 472–478.
13. VAN SNICK, J., CAYPHAS, S., VINK, A., UYTTENHOVE, C., COULIE, P.G., RUBIRA, M.R., and SIMPSON, R.J. (1986). Purification and NH_2-terminal amino acid sequence of a T-cell-derived lymphokine with growth factor activity for B-cell hybridomas. Proc. Natl. Acad. Sci. USA **83**, 9679–9683.
14. COX, R.A., and SMULIAN, N.J. (1983). A single step procedure for the isolation of individual mRNA species from crude lysates of physarum polycephalum. FEBS Lett. **155**, 73–80.
15. PALIARD, X., DE WAAL MALEFIJT, R., YSSEL, H., BLANCHARD, D., CHRETIEN, I., ABRAMS, J., DE VRIES, J., and SPITS, H. (1988). Simultaneous production of IL-2, IL-4, and IFN-γ by activated human $CD4^+$ and $CD8^+$ T cell clones. J. Immunol. **141**, 849–855.
16. KOVACS, E.J., RADZIOCH, D., YOUNG, H.A., and VARESIO, L. (1988). Differential inhibition of IL-1 and TNF-α mRNA expression by agents which block second messenger pathways in murine macrophages. J. Immunol. **141**, 3101–3105.
17. KELSO, A., and GOUGH, N.M. (1988). Coexpression of granulocyte-macrophage colony-stimulating factor, γ interferon and interleukin 3 and 4 is random in murine alloreactive T-lymphocyte clones. Proc. Natl. Acad. Sci. USA **85**, 9189–9193.
18. TOVEY, M.G., CONTENT, J., GRESSER, I., GUGENHEIM, J., BLANCHARD, B., GUYMARHO, J., POUPART, P., GIGOU, M., SHAW, A., and FIERS, W. (1988). Genes for

IFN-β_2 (IL-6), tumor necrosis factor, and IL-1 are expressed at high levels in the organs of normal individuals. J. Immunol. **141**, 3106–3110.

19. VAN DER KORPUT, J.A.G.M., HILKENS, J., KROEZEN, V., ZWARTHOFF, E.C., and TRAPMAN, J. (1985). Mouse interferon alpha and beta genes are linked at the centromere proximal region of chromosome 4. J. Gen. Virol. **66**, 493–502.
20. MOCK, B.A., NORDAN, R.P., JUSTICE, M.J., KOZAK, C., JENKINS, N.A., COPELAND, N.G., CLARK, S.C., WONG, G.G., and RUDIKOFF, S. (1989). The murine IL-6 gene maps to the proximal region of chromosome 5. J. Immunol. **142**, 1372–1376.
21. HARADA, H., FUJITA, T., MIYAMOTO, M., KIMURA, Y., MARUYAMA, M., FURIA, A., MIYATA, T., and TANIGUCHI, T. (1989). Structurally similar but functionally distinct factors, IRF-1 and IRF-2, bind to the same regulatory elements of IFN and IFN-inducible gene. Cell **58**, 729–739.
22. RAY, A., TATTER, S.B., MAY, L.T., and SEHGAL, P.B. (1988). Activation of the human "β_2-interferon/hepatocyte-stimulating factors/interleukin 6" promoter by cytokines, viruses, and second messenger agonists. Proc. Natl. Acad. Sci. USA **85**, 6701–6705.
23. TANABE, O., AKIRA, S., KAMIYA, T., WONG, G.G., HIRANO, T., and KISHIMOTO, T. (1988). Genomic structure of the murine IL-6 gene. High degree conservation of potential regulatory sequences between mouse and human. J. Immunol. **141**, 3875–3881.
24. VISVANATHAN, K.V., and GOODBOURN, S. (1989). Double-stranded RNA activates binding of NF-κB to an inducible element in the human β-interferon promoter. EMBO J. **8**, 1129–1138.

Address reprint requests to:
Dr. Istvan Rosztoczy
Institute of Microbiology
Albert Szent-Gyorgyi Medical University
Dom ter 10, H-6720
Szeged, Hungary

Received 8 August 1990/Accepted 13 September 1991

III.

MOLECULAR AND CELLULAR BIOLOGY, Apr. 1995, p. 2207–2218
0270-7306/95/$04.00+0

Vol. 15, No. 4

Stimulation of Interferon and Cytokine Gene Expression by Imiquimod and Stimulation by Sendai Virus Utilize Similar Signal Transduction Pathways†

KLARA MEGYERI,[1]‡ WEI-CHUN AU,[1] ISTVAN ROSZTOCZY,[1] N. BABU K. RAJ,[1] RICHARD L. MILLER,[2] MARK A. TOMAI,[2] AND PAULA M. PITHA[1,3]*

Oncology Center[1] and Department of Molecular Biology and Genetics,[3] The Johns Hopkins University School of Medicine, Baltimore, Maryland 21231, and Department of Pharmacology, 3M Pharmaceuticals, St. Paul, Minnesota 55144[2]

Received 19 September 1994/Returned for modification 31 October 1994/Accepted 27 January 1995

The imidazoquinolineamine derivative 1-(2-methyl propyl)-1*H*-imidazole [4,5-*c*]quinoline-4-amine (imiquimod) has been shown to induce alpha interferon (IFN-α) synthesis both in vivo and in peripheral blood mononuclear cells in vitro. In this study, we show that, in these cells, imiquimod induces expression of several *IFNA* genes (*IFNA1*, *IFNA2*, *IFNA5*, *IFNA6*, and *IFNA8*) as well as the *IFNB* gene. Imiquimod also induced the expression of interleukin (IL)-6, IL-8, and tumor necrosis factor alpha genes. Expression of all these genes was transient, independent of cellular protein synthesis, and inhibited in the presence of tyrosine kinase and protein kinase C inhibitors. Infection with Sendai virus led to expression of a similar set of cytokine genes and several of the *IFNA* genes. Imiquimod stimulates binding of several induction-specific nuclear complexes: (i) the NF-κB-specific complexes binding to the κB enhancer present in the promoters of all cytokine genes, but not in *IFNA* genes, and (ii) the complex(es) binding to the A4F1 site, 5′-GTAAAGAAAGT-3′, conserved in the inducible element of *IFNA* genes. These results indicate that imiquimod, similar to viral infection, stimulates expression of a large number of cytokine genes, including IFN-α/β, and that the signal transduction pathway induced by both of these stimuli requires tyrosine kinase and protein kinase activity.

The low-molecular-weight imidazoquinolineamine derivative 1-(2-methyl propyl)-1*H*-imidazole [4,5-*c*]quinoline-4-amine (imiquimod) inhibits replication of herpes simplex virus type 2 and cytomegalovirus in infected guinea pigs (6, 24). Imiquimod-mediated inhibition of virus replication is related to its ability to induce interferon (IFN). Oral administration of imiquimod induces IFN-α in mice, rats, guinea pigs, monkeys, and humans. (New approved nomenclature for IFN genes [9a] is used throughout this paper.) In addition to having antiviral activity, imiquimod was shown to inhibit growth of several transplantable murine tumors, including MC-26 colon carcinoma and Lewis lung carcinoma (71). The induction of IFN-α plays a major, but not exclusive, role in this growth inhibition, since an antiserum to mouse IFN-α and IFN-β significantly reduced the antitumor effect of imiquimod but was not able to abolish it completely.

IFN-α proteins are represented by a large family of structurally related genes which show about 94% homology at the nucleotide level, while IFN-β is encoded by a single gene. *IFNA* genes are expressed preferentially in cells of lymphoid lineage, and the individual subtypes show cell-type-specific differences in expression (2, 29, 35), while *IFNB* is expressed in a large variety of cells. The biological significance of the large abundance of *IFNA* genes is not clear; all IFN-α and IFN-β subtypes show antiviral and antitumor properties and seem to bind to a common receptor (39); however, some differences between their immunomodulatory effects have been reported (21, 56).

Virus-induced expression of *IFNA* and *IFNB* genes is mediated by a virus-responsive element (VRE) present in the promoters of *IFNA* and *IFNB* genes that, by itself, functions as a virus-specific enhancer and can confer inducibility in infected cells (3, 14, 19, 20, 58, 65). At least two families of transcriptional factors were shown to play a role in induction of IFN genes that have binding sites within the VRE. One family is the set of IFN-responsive factors IRF-1 and IRF-2, which function as activator and repressor, respectively (22, 23). Overexpression of these two factors can regulate activity of both *IFNA* and *IFNB* promoter regions in a transient expression assay; a single nucleotide mutation in the IRF-1 binding site of the murine *IFNA4* gene promoter decreased inducibility by about 100-fold (2), and cells expressing IRF-1 antisense mRNA were unable to express *IFNB* genes (62). However, the role of IRF-1 in induction of the IFN gene has been questioned, since deletion of the IRF-1 gene did not affect virus-mediated inducibility of IFN genes either in mice in vivo or in cultured cells in vitro (53, 64). The second family of transcriptional factors are the κB-specific binding proteins that play a role in activation of the *IFNB* gene (16, 19, 28, 43, 77), and recently, a direct role of IFN-induced double-stranded RNA (dsRNA)-dependent kinase in activation of NF-κB has been shown (37, 49). Furthermore, it was shown that HMG I(Y) and ATF-2 can bind to the VRE (48, 75) of the *IFNB* gene, where HMG I(Y) proteins appear to bend the DNA and facilitate binding of both NF-κB and ATF-2.

Factors involved in the regulation of *IFNA* genes other than IRF-1 are less well-defined. Two proteins of 68 and 96 kDa were found to bind the A4F1 regulatory element in the VRE of the murine *IFNA4* gene promoter (1, 2), and MacDonald et al.

* Corresponding author. Mailing address: The Johns Hopkins University, Oncology Center, 418 N. Bond St., Baltimore, MD 21231-1001. Phone: (410) 955-8871. Fax: (410) 955-0840. Electronic mail address: parowe@welchlink.welch.jhu.edu.

† This paper is dedicated to the memory of Istvan Rosztoczy, who initiated this work and who died in October 1993 while climbing Mount Fuji in Japan.

‡ Present address: Mikrobiologiai Intezet, Szent-Györgyi Albert Orvostudományi Egyetem, H-6720 Szeged, Hungary.

(47) described a factor (named TG) that binds to the VRE of the human *IFNA1* gene. These proteins, however, have not yet been characterized.

The signal transduction pathway, triggered by viral infection that activates these factors and leads to the induction of IFN genes, is not known. Earlier studies have suggested that the dsRNA formed as an intermediate product during replication of RNA viruses is essential for the stimulation of expression of IFN genes (32, 50). This assumption was based on the following observations. First, there is a difference in the IFN-inducing capacities of plus- and minus-stranded RNA viruses. Infectivity of plus-stranded viruses is essential for IFN induction, while the ability of UV-irradiated minus-stranded viruses to induce IFN correlated with their ability to transcribe their genome and produce complementary RNA (26, 46). Second, D1 particles of vesicular stomatitis virus containing covalently linked complementary message and antimessage RNA are very effective IFN inducers (51) and dsRNA, such as poly(rI)·poly(rC), alone is able to induce expression of the *IFNB* gene (11). Third, DNA viruses that do not form dsRNA during the replication cycle are not effective inducers of IFN (30). However, in lymphocytes, expression of the Sendai virus C gene was sufficient to induce IFN (74), and viral glycoproteins or nucleic acid-free viral envelopes were also able to induce IFN production in peripheral blood mononuclear cells (PBMC) (12, 33, 40, 42, 81). Thus, the role of dsRNA as an essential trigger for IFN induction remains questionable.

The aim of the proposed study was to analyze the molecular mechanism by which imiquimod (R-837) stimulates IFN synthesis in PBMC in vitro, to determine the responsive cell type(s), and to identify the expressed IFN subtypes. The results show that imiquimod stimulates expression of *IFNA1*, *IFNA2*, *IFNA5*, *IFNA6*, and *IFNA8* genes as well as *IFNB* in PBMC and that IFN synthesis can be detected in B cells and monocytes/macrophages. In addition to inducing expression of IFN genes, imiquimod also induced expression of tumor necrosis factor alpha (TNF-α), interleukin-6 (IL-6), and IL-8 genes; expression of all these genes was transient, independent of cellular protein synthesis, and inhibited by tyrosine kinase (TK) and protein kinase C (PKC) inhibitors.

MATERIALS AND METHODS

Isolation of different populations of leukocytes. Human PBMC were isolated from Leukopack platelets by density gradient centrifugation in lymphocyte separation medium (LSM) (Organon Teknika Corp., Durham, N.C.) (4). The cells were further separated on the basis of their adherence to plastic surfaces (36). To determine the type of cells responsible for IFN production, B cells, T cells, and monocytes were isolated either by sorting with a fluorescence-activated cell sorter (FACS) or by indirect rosetting with Dynabeads. T and B lymphocytes were separated by FACS from the nonadherent population of human PBMC after being stained with anti-Leu-4 (CD3) and anti-Leu-12 (CD19) monoclonal antibodies, respectively (Simultest T and B Cell Test; Becton-Dickinson). For separation by magnetic beads, T cells and B cells were first isolated from the nonadherent fraction of PBMC by rosetting with sheep erythrocytes as described elsewhere (13). T cells were then isolated by positive selection with anti-CD3 monoclonal antibody and incubated with anti-mouse-immunoglobulin G (IgG)-coated Dynabeads. B cells consisted of a population of a nonadherent, E-rosette-negative fraction of PBMC that did not form rosettes with the anti-mouse-IgG-coated dynabeads after treatment with anti-CD3 and anti-CD14 murine monoclonal antibodies. Monocytes were isolated from a fraction of human PBMC that adhered (after 15 min) to plastic by staining with anti-CD14 mouse monoclonal antibody and selection with anti-mouse-IgG-coated Dynabeads. For induction, 5×10^6 PBMC, monocytes, or nonadherent cells per ml and 5×10^4 separated cells per ml were used. Cells were cultured in RPMI 1640 medium supplemented with 10% fetal bovine serum and 2 mM L-glutamine.

PCR analysis. Two sets of oligonucleotide primers corresponding to sequences of human *IFNA* genes were used (25). A pair of primers designed to recognize all of the *IFNA* subtypes had the following sequences: 5′ primer, GTACTGCAGAATCTCTCCTTTCTCCTG (nucleotides [nt] +1067 to 1086); 3′ primer, GTGTCTAGATCTGACAACCTCCCAGGGCACA (nt +1415 to 1435). The second set of primers was specific for *IFNA2* and had the following sequences: 5′ primer, GTACTGCAGCATCTGCAACATCTAC (nt +911 to 930); 3′ primer, GTGTCTAGAGTCTTTGAAATGGCAG (nt +1565 to 1582). The general primers, selected from a highly conserved region of the *IFNA* genes (see Fig. 4), amplified a 369-bp fragment, while the *IFNA2*-specific primers amplified a 672-bp product corresponding predominantly to *IFNA2* mRNA. Each primer contained either a *PstI* (5′ primer) or an *XbaI* (3′ primer) restriction sequence that facilitated its cloning. The sequences of the restriction sites are underlined; a single line represents the *PstI* site, and a double line represents the *XbaI* site.

In the reverse transcription (RT)-PCR analysis, first-strand synthesis (cDNA) was carried out in 50 mM Tris-HCl (pH 8.3)–140 mM KCl–10 mM $MgCl_2$–4 mM dithiothreitol (DTT)–1 mM each deoxynucleoside triphosphate (dNTP mix)–20 U of RNase inhibitor (Life Technologies, Inc.)–1.25 U of avian myeloblastosis virus reverse transcriptase (Life Technologies, Inc.)–1 μg of oligo(dT) (Sigma). The reaction mixture (25 μl) was incubated at 42°C for 2 h. Next, 1/10 of the cDNA mixture was amplified in 50 mM KCl–10 mM Tris-HCl (pH 8.3)–1.5 mM $MgCl_2$–0.01% (wt/vol) gelatin–200 μM dNTP mix–200 μg of each primer–2.5 U of *Taq* DNA polymerase (Boehringer Mannheim, Indianapolis, Ind.) in a volume of 50 μl by use of an automated thermocycler (Perkin-Elmer Cetus, Norwalk, Conn.). Reaction mixtures were heated to 94°C for 4 min and subjected to 30 amplification cycles, each consisting of three rounds at 94, 50, and 72°C, respectively, for 1 min each followed by a final extension for 5 min at 72°C. As a control, amplifications were done in a reaction mixture without first-strand cDNA. Amplified fragments were either digested with the appropriate restriction endonucleases to identify the fragment amplified or ligated to pGEM4.

DNA sequencing. Sequencing of dsDNA was done by the dideoxy chain-terminating method (68) with a Sequenase kit (United States Biochemical Corp.) and SP6 and T7 primers.

RNA and DNA probes. *IFNA* riboprobe was prepared by insertion of a 764-bp *EcoRI-BglII* fragment of human *IFNA2* cDNA (55) into pSP64 followed by cloning. The plasmid was linearized with *EcoRI*, and RNA was transcribed by SP6 polymerase. The *IFNB* probe was prepared by insertion of a 520-bp fragment of human *IFNB* cDNA (60) into pSP64, and the plasmid was linearized with *EcoRI*. The IL-6 probe was prepared by insertion of a 550-bp *PstI* fragment of human IL-6 cDNA into pSP64 vector, followed by linearization with *EcoRI*. IRF-1 probe was prepared by ligation of a 460-bp *BglI-EcoRI* fragment of human IRF-1 cDNA into the *HincII* site of pSP65 and linearization with *HindIII*. TNF-α probe was represented by an 800-bp *EcoRI* fragment of human TNF-α cDNA in Bluescript SK vector; after linearization with *BamHI*, RNA was transcribed with T7 polymerase. Human γ-actin cDNA in pSP64 vector was linearized with *HinfI*. All transcribed RNAs were radiolabelled with [α-^{32}P]GTP as described previously (1). pTZ/IL-8 plasmid was digested with *PstI*, and the ~400-bp cDNA insert was purified and labelled with [α-^{32}P]dCTP (Pharmacia) by random priming.

Northern (RNA) blot analysis. Human PBMC (10^7 per cell sample) were stimulated with 3 μg of imiquimod per ml or infected with Sendai virus for various times; control cultures incubated in parallel were left untreated. Total cellular RNA was prepared by the guanidine thiocyanate method (7), and 10 μg was denatured in 50% deionized formamide–2.2 M formaldehyde–20 mM MOPS (morpholinepropanesulfonic acid) for 15 min at 60°C and chilled on ice. RNA was then fractionated by electrophoresis in 0.8% agarose gels containing 2.2 M formaldehyde and 20 mM MOPS and subsequently blotted onto nitrocellulose filters with 20× SSC (1× SSC is 0.15 M NaCl plus 0.015 M sodium citrate). Prehybridization and hybridization with single-stranded riboprobes or dsDNA probes were performed at 60 and 45°C, respectively, in a buffer containing 50% formamide, 0.1% sodium dodecyl sulfate (SDS), 5× SSC, 1× Denhardt's solution, 50 mM potassium phosphate buffer (pH 6.6), and 0.25 μg of denatured salmon sperm DNA per ml. After hybridization, filters were washed with 0.1% SDS–0.5× SSC at 60 or 45°C and exposed to Kodak XAR-5 film with intensifying screens at −70°C. Blots were stripped for sequential hybridization by boiling with 0.1× SSC–0.1% SDS for 15 min.

Preparation of nuclear extracts. Nuclear extracts were prepared as described previously (2), and specific protein-DNA complexes were detected by a gel mobility shift assay (2). Briefly, each cell pellet was resuspended in buffer A (10 mM *N*-2-hydroxyethylpiperazine-*N*′-2-ethanesulfonic acid [HEPES] [pH 7.9], 1.5 mM $MgCl_2$, 10 mM KCl, 0.3 mM DTT, 0.5 mM phenylmethylsulfonyl fluoride [PMSF], and 0.5% Nonidet P-40) and incubated at 4°C. Nuclei were collected by centrifugation, resuspended in buffer C (20 mM HEPES [pH 7.9], 25% glycerol, 500 mM KCl, 1.5 mM $MgCl_2$, 0.2 mM EDTA, 0.5 mM DTT, 0.5 mM PMSF), and incubated for 30 min at 4°C. After centrifugation at 15,000 rpm in a Tomy MTX-150 microcentrifuge, the supernatant fraction was dialyzed against buffer D (20 mM HEPES [pH 7.9], 50 mM KCl, 0.2 mM EDTA, 20% glycerol, 0.5 mM DTT, 0.5 mM PMSF) and stored at −70°C.

Preparation of radiolabelled oligonucleotides and electrophoretic mobility shift assays. Double-stranded oligonucleotide spanning the NF-κB site of human immunodeficiency virus type 1 (HIV-1) long terminal repeat (LTR) (5′-TCAAGGGACTTTCCGCTGGGACTTTCCCTCTCCTT-3′) (78) was used for DNA binding studies. The underlined sequence was used for annealing of a primer, GGGAGAGGAA, and synthesis of the complementary strand with Klenow polymerase labelled with [^{32}P]dCTP. Protein-DNA complexes were formed by incubation of 5 to 10 μg of nuclear protein with 1 to 10 pg of radiolabelled DNA probe at 4°C for 5 min in a 25-μl reaction volume containing 12 mM Tris (pH 7.6), 100 mM KCl, 0.1 mM EDTA, 0.5 mM DTT, 5 mM $MgCl_2$ 2 μg of poly(dI)·poly(dC) per ml, and 7% glycerol. For supershift experiments,

TABLE 1. Induction of IFN synthesis in R-837-stimulated and Sendai virus-infected PBMC

Cell type	No. of Sendai virus-infected cells at 16 h	Amt of IFN (U/ml) induced by imiquimod at:						
		0 h	2 h	3 h	4 h	5 h	9 h	24 h
Unseparated[a]	5×10^3	<2	<2	160	ND[b]	1,280	192	2
Monocytes	8×10^3	<2	<2	8	ND	16	6	16
Nonadherent	6×10^3	<2	16	2,048	640	256	128	28
$CD14^+$ monocytes[c]	256						6	6
$CD18^+$ B cells[a]	128						32	
$CD3^+$ T cells[a]	<4						<4	

[a] 5×10^6 cells per ml were used for stimulation.
[b] ND, not done.
[c] Cells were separated by FACS; separation with Dynabeads gave similar results. 5×10^4 cells per 100 μl were used for stimulation.

serum containing antibodies against p65, p50, or c-rel was added to the preincubated DNA-protein binding mixture and then the mixture was incubated for 1 h on ice.

The sequences of A4F1 (2) and PRDI (48) used as probes were 5'-GCGTA AAGAAAGTCCCTCTCCTT and 5'-GAGAAGTGAAAGTGGGAACCCTC TCCTT, respectively; the primer-annealing sequence is underlined. The ^{32}P-labelled double-stranded probes were prepared by extension of the primer with Klenow polymerase and [^{32}P]dCTP. The binding mixture was identical to that described above.

Protein-DNA complexes were resolved by electrophoresis on 4% nondenaturing polyacrylamide gels in 0.4× Tris-borate-EDTA, pH 8.3, at 150 V for 2 h at room temperature. Gels were dried and exposed to Kodak X-ray film.

UV cross-linking in situ. Nuclear proteins were bound to a probe (A4IE) that corresponds to the virus-inducible element of the *IFNA4* gene promoter region containing the A4F1 and IRF-1 binding sequences (2) substituted with 5'-bromo-2'-deoxyuridine (BrdUrd) (Boehringer-Mannheim) and labelled with Klenow polymerase and [^{32}P]dCTP. The DNA-protein complex was resolved on a 4% nondenaturing polyacrylamide gel and UV irradiated in situ for 10 min at 4°C (2, 78). The UV-cross-linked DNA-protein adduct was then eluted and separated on an SDS–10% acrylamide gel.

RESULTS

Induction of IFN in human PBMC. To determine the kinetics of IFN production in human PBMC, cells were induced with 3 μg of imiquimod per ml for different periods of time. The applied dose was found to be optimal in a dose-response experiment (data not shown). Imiquimod induced rapid and transient IFN production, with the highest yield between 3 and 5 h after induction (Table 1). In contrast, the maximal response to Sendai virus infection was observed between 10 and 12 h postinduction (data not shown) and synthesis proceeded for about 24 h (Table 1 and data not shown). The IFN was identified as human IFN-α by serologic characterization, since 98% of the antiviral activity was neutralized by antibodies to human IFN-α. In addition to inducing IFN, both imiquimod and Sendai virus induced high levels of IL-6 (6,400 U at 4 h).

Identification of the cell types producing IFN-α. To evaluate the phenotype of the IFN-producing cells in human PBMC, we initially separated PMBC into a population of cells that adhered to plastic (the majority of cells are monocytes) and those that were nonadherent (predominantly B and T cells) and found that both these cell populations produced IFN-α after exposure to imiquimod. We therefore further purified B cells, T cells, and monocytes by FACS sorting or indirect rosetting with dynabeads as described in Materials and Methods. Separated cells were induced with imiquimod or Sendai virus, and medium was assayed for IFN activity (Table 2). Both Sendai virus and imiquimod induced IFN synthesis in B cells and monocytes but not in T cells. Thus, for the producer cell types, there was no difference between Sendai virus and imiquimod.

Imiquimod-induced expression of *IFNA*, *IFNB*, TNF-α, IL-6, IL-8, and IRF-1 mRNAs. We further examined the effect of imiquimod treatment on expression of IFN genes and analyzed the relative levels of *IFNA* and *IFNB* mRNAs in stimulated cells. The results of Northern blot analysis are shown in Fig. 1. Stimulation with imiquimod led to a significant increase in the relative levels of *IFNA* and *IFNB* mRNAs as early as 2 h after induction, while at 6 h poststimulation *IFNA* and *IFNB* mRNAs were undetectable. Although we did not detect IFN-β protein, Northern blot analysis revealed the presence of *IFNB* mRNA in induced cells. *IFNB* mRNA was stabilized in the presence of cycloheximide (CHX) as described previously (60, 61) (Fig. 1). Expression of the *IFNB* gene without detectable secretion of the IFN-β protein has previously been found to occur in Sendai virus-induced Namalwa cells (59, 70).

Imiquimod stimulation of PMBC also increased the relative levels of TNF-α, IL-6, and IL-8. Expression of all these genes was transient, reaching a maximum between 2 and 4 h after induction and decreasing to baseline levels at 24 h. Expression of the transcription factor IRF-1, which is induced by viral infection, showed slower kinetics; maximal levels of IRF-1 mRNA were detected at 4 h after induction, and expression did not return to baseline levels over 12-h period. It has been shown that both TNF-α and IFNs induce expression of IRF-1 mRNA (15); thus, the prolonged increase in IRF-1 levels observed may be mediated by the cytokines induced by imiquimod. Imiquimod-stimulated expression of all these cytokine genes did not require ongoing protein synthesis, and increased levels of the respective cytokine mRNAs could be detected in CHX-treated cells. CHX was previously shown to increase the rate of *IFNB* transcription by interfering with synthesis of the

TABLE 2. Induction of IFN-α in different cell types

Selection method and cell type[a]	Amt of IFN (U/ml)[b] induced by:	
	Imiquimod	Sendai virus
FACS selection		
Monocytes ($CD14^+$)	14	64
B cells ($CD19^+$)	16	128
T cells ($CD3^+$)	<2	<2
Dynabead selection		
Monocytes ($CD14^+$) (adherent)	6	256
B cells ($CD3^-$ $CD14^-$) (nonadherent, E-rosette negative)	32	ND
T cells ($CD3^+$) (nonadherent, E-rosette positive)	<4	<4

[a] 5×10^4 separated cells were used for induction; uninduced cells produced less than 4 U of control activity per ml.
[b] Antiviral activity was abolished by treatment with antibodies to human IFN-α.

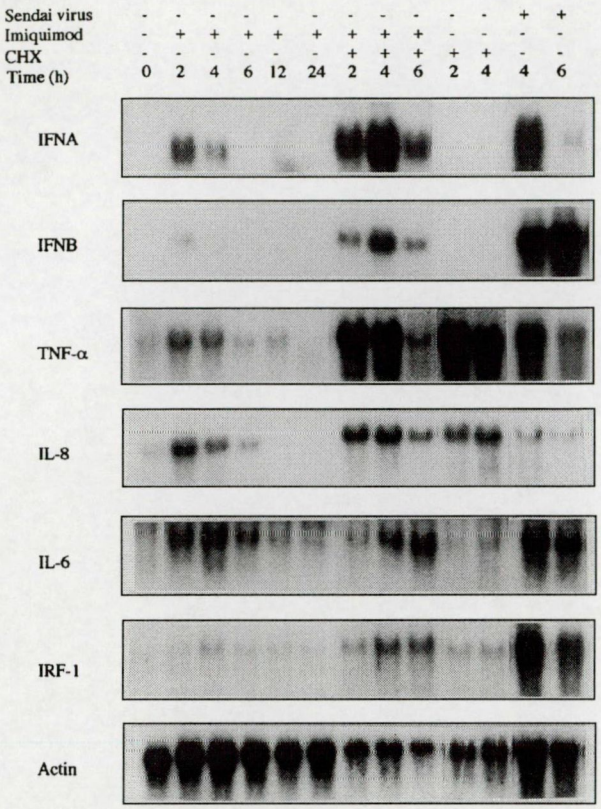

FIG. 1. Expression of IFN-α/β, TNF-α, IL-6, IL-8, and IRF-1 genes in imiquimod-stimulated PBMC. PBMC isolated on a Ficoll gradient were induced (2×10^7 cells per sample) with imiquimod (3 μg/ml) in the presence (+) and absence (−) of CHX (30 μg/ml) for the indicated times. Isolated total RNA (10 μg) was analyzed by Northern hybridization with the respective probe as described in Materials and Methods. As a control, cells were induced with 200 hemagglutinin units of Sendai virus per ml for 4 and 6 h. Films were exposed for 16 h. Hybridization with γ-actin probe is shown as a control for RNA loading.

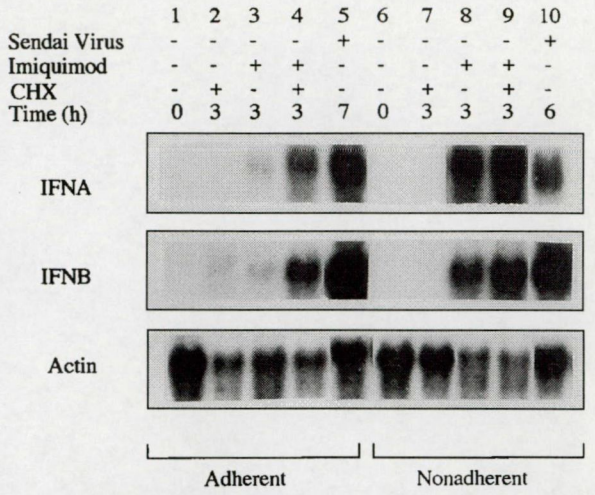

FIG. 2. Expression of *IFNA* and *IFNB* genes in induced adherent and nonadherent PBMC. PBMC were allowed to adhere to plastic for 50 min; nonadherent cells were collected, and adherent cells were washed with medium containing 1% fetal bovine serum. Induction was done for 3 h with imiquimod-stimulated cells (lanes 3 and 8) and for 6 to 7 h with Sendai virus-infected cells (lanes 5 and 10). Cells treated with CHX alone or CHX in combination with imiquimod are shown in lanes, 2, 4, 7, and 9. Isolation and analysis of total RNA were done as described in the legend to Fig. 1. A 16-h exposure of the membranes is shown. Lanes 1 to 5 represent adherent cells, and lanes 6 to 10 represent nonadherent cells. +, present; −, absent.

transcriptional repressor (34) as well as activating NF-κB (p50-p65 complex) (27, 69), which may lead to increased transcription of TNF-α, IL-6, and IL-8 genes, as well as *IFNB*. Furthermore, the posttranscriptional effect of CHX, which occurs at the level of mRNA stabilization, was demonstrated for *IFNB* and TNF-α (45, 60).

Induction of IFN genes and various cytokine genes in Sendai virus-infected PBMC was analyzed as a control. Sendai virus induced expression of all these cytokine genes; however, two major differences between imiquimod and Sendai virus were observed: (i) Sendai virus-induced expression of these genes was slow; maximal increases in the *IFNA* and *IFNB* mRNA levels occurred at 4 and 6 h postinfection, respectively; and (ii) Sendai virus was a more effective inducer of all cytokine genes, except the IL-8 gene, which was induced more effectively by imiquimod.

The levels of *IFNA* and *IFNB* mRNAs were further analyzed with stimulated populations of adherent cells enriched with monocytes and macrophages and nonadherent cells containing mostly T and B cells. A significant increase in the relative levels of *IFNA* and *IFNB* mRNAs after imiquimod treatment was observed to occur in both imiquimod-stimulated and Sendai virus-infected adherent and nonadherent cells (Fig. 2). These results are in agreement with those from analyses of biologically active IFNs which were shown to be produced in both adherent and nonadherent cells (Table 1).

Imiquimod does not stimulate expression of *IFNA/B* and IL-6 genes in murine monocyte line Raw but alters the NDV-mediated stimulation of these genes. We have not been able to induce expression of IFN-α/β genes by imiquimod in any fibroblast, B-cell, T-cell, or monocyte line tested (data not shown). However, we have been able to induce effectively the expression of various cytokine genes in the murine macrophage line Raw 264, both by viral infection and by treatment with lipopolysaccharide. We have, therefore, tested whether imiquimod induces expression of *IFNA/B* and cytokine genes in these cells. While no stimulation of *IFNA*, *IFNB*, or the IL-6 gene could be induced by imiquimod in these cells, treatment with imiquimod during virus infection significantly inhibited the Newcastle disease virus (NDV)-mediated induction of *IFNA* genes (Fig. 3A). In contrast, treatment with imiquimod superinduced NDV-induced *IFNB* mRNA levels by about 2- to 3-fold and IL-6 mRNA levels by about 10-fold. These results show that, in the absence of detectable stimulation of *IFNA/B* and IL-6 genes, imiquimod differentially altered the expression of *IFNA* and *IFNB* or IL-6 genes.

To determine whether these effects can also be seen in cells where imiquimod induces expression of cytokine genes, PBMC were infected with NDV in the presence of imiquimod. The relative levels of *IFNA* mRNA were lower in cells treated with both inducers than in those induced with NDV alone. The presence of *IFNA* mRNA could also be detected in cells treated with imiquimod alone (Fig. 3), although the levels were much lower than those induced by NDV, since maximal levels of *IFNA* mRNA in imiquimod-treated cells are induced at 2 h postinfection (compare Fig. 1). These data indicate that imiquimod has a noticeable inhibitory effect on the NDV-stimulated expression of *IFNA* genes in both human PBMC and the

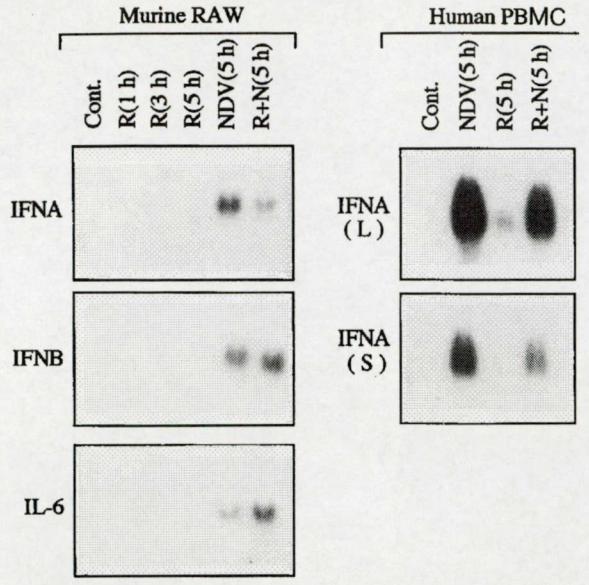

FIG. 3. Imiquimod modulates NDV-mediated induction of IFN and IL-6 genes. Murine Raw 264 cells at 80% confluency and human PBMC were induced with imiquimod (R) (3 μg/ml) for the indicated periods of time, after which total RNA was isolated. Alternatively, these cells were induced with NDV (N) (multiplicity of infection of 5) in the presence and absence of imiquimod (3 μg/ml) for 5 h. Total RNA (10 μg) was analyzed by Northern hybridization as described in Materials and Methods. A 20-h exposure of the films is shown in panel IFNA (L), and a 4-h exposure is shown in panel IFNA (S). Cont., control; L, long; S, short.

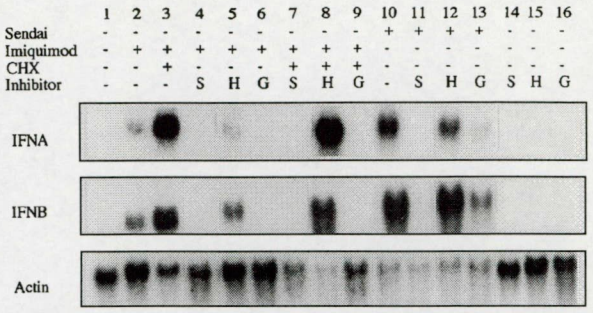

FIG. 4. Inhibition of imiquimod-mediated induction of *IFNA* and *IFNB* genes by genistein (G) and staurosporin (S). PBMC were pretreated with genistein (100 nM), staurosporin (80 nM), or HA1004 (H) (30 μM) for 30 min and then induced with imiquimod or Sendai virus in the presence or absence of an inhibitor. RNA was isolated at 3 h postinduction with imiquimod (lanes 2 to 9) or at 6 h postinfection with Sendai virus (lanes 10 to 13) and analyzed by Northern hybridization with *IFNA* and *IFNB* probes as described in Materials and Methods. Hybridization with γ-actin probe was used to estimate the amounts of RNA on filters. +, present; −, absent.

murine macrophage line Raw. Similar to what was observed with murine Raw cells, no inhibition in the *IFNB* and IL-6 mRNAs was seen after treatment with virus and imiquimod (data not shown). These data suggest that the virus-induced signal transduction pathways that lead to the induction of *IFNA* and *IFNB* genes are not identical.

Effect of kinase inhibitors on expression of IFN genes. To determine whether induction of *IFNA* and *IFNB* genes by imiquimod and induction by Sendai virus occur through similar signal transduction pathways, we analyzed the effects of inhibitors of TK, PKC, and protein kinase A (PKA) on stimulation of *IFNA* and *IFNB* gene expression in induced cells. Figure 4 shows that treatment of the cells with staurosporin (PKC inhibitor) and genistein (TK inhibitor), before and during induction, resulted in inhibition of *IFNA* and *IFNB* expression, and no *IFNA* or *IFNB* mRNA could be detected in cells 2 h postinduction (lanes 4, 6, and 7). Additional experiments in which we used calphostin C, a more specific inhibitor of PKC, also showed that pretreatment with 50 nM calphostin C completely inhibited induction of *IFNA* (data not shown), thus indicating that PKC activity is required for the induction process. In contrast, treatment with HA1004 (PKA inhibitor) did not significantly change levels of *IFNA* and *IFNB* mRNAs induced by either Sendai virus or imiquimod (Fig. 4, lanes 5 and 12). These results suggest that both TK and PKC activity, but not PKA, are part of the imiquimod-mediated transduction signal. When the effect of these inhibitors on Sendai virus-mediated induction of *IFNA* and *IFNB* genes was examined, staurosporin and genistein, but not HA1004, were found to inhibit the appearance of *IFNA* and *IFNB* mRNAs in infected cells (Fig. 4, lanes 11 to 13). However, while staurosporin was able to completely block induction of *IFNA* mRNAs, low levels of *IFNA* and *IFNB* mRNAs could still be detected in genistein-treated cells, suggesting that genistein is a less effective inhibitor of virus-mediated induction than is staurosporin.

Similar results were observed when the effect of these inhibitors on expression of IL-6, IL-8, and TNF-α genes was examined (data not shown). Both genistein and staurosporin, but not HA1004, inhibited the imiquimod- and virus-induced expression of these genes. In contrast, there was little variation in the relative levels of actin mRNA induced in the presence and absence of inhibitors, showing that the effect is specific and is not due to toxicity or variations in RNA loading. These data, together with lack of dependence of induction of *IFNA* and *IFNB* genes on cellular protein synthesis, suggest that induction of IFN genes by both virus infection and imiquimod involves phosphorylation of preexisting cellular factors.

Determination of *IFNA* subtypes induced by imiquimod. The high degree of homology among *IFNA* genes prevents identification of various *IFNA* mRNA subtypes by Northern blot hybridization. We and others have previously used S1 and RNase protection analyses for identification of various *IFNA* mRNAs in infected murine and human cells (29, 35). In the present study, we used a more sensitive RT-PCR assay. Total cellular RNA isolated from PBMC induced by imiquimod or by Sendai virus was used as a template for reverse transcription of *IFNA*-specific transcripts. The IFN cDNAs were then amplified by PCR, and the amplified DNA was characterized by restriction analysis, cloned, and sequenced.

Two sets of primers were used for amplification of the cDNAs (Fig. 5). Initially, primers containing highly conserved sequences (general primers) were used (see Materials and Methods) and PCR-amplified DNA fragments were analyzed by restriction with *Ava*II and *Ava*I endonucleases, which are specific for *IFNA1* and *IFNA4*, respectively. After restriction of the amplified DNA fragment (369 nt) from both Sendai virus- and imiquimod-induced cDNAs with *Ava*II, two small fragments of 171 and 188 bp were detected, indicating the presence of *IFNA1* transcripts in these cells (Fig. 6A). However, the density of these restriction fragments indicated that the levels of *IFNA1* transcripts in imiquimod-induced cells were much lower than those in Sendai virus-induced cells. In contrast, the amplified DNA fragments were not restricted with *Ava*I, indicating the absence of *IFNA4* transcripts in Sendai virus- and imiquimod-induced cells. The amplified fragment from both

5' primer (coding strand) 3' primer (noncoding strand)

High conservation of sequences used as PCR primers

IFN A1	.....AGAATCTCTC CTTcCTCCTG TCTG.....	.....CTGC TCTGACAACC TCCCAGGCAC.....
IFN A2	.....AGAATCTCTC tTTTCTCCTG CTTG.....	.....CTGC TCTGACAACC TCCCAGGCAC.....
IFN A4	.....AGAATCTCTC aTTTCTCCTG CCTG.....	.....CTGC TCTGACAACC TCCCAGGCAC.....
IFN A5	.....AGAATCTCTC CTTTCTCCTG CCTG.....	.....CTGA TCTGTCAACC TCCCAtGCAC.....
IFN A6	.....AGAATCTCTC tTTTCTCCTG TCTG.....	.....CTGA TCTGTCAACC TCCCAGGCAC.....
IFN A7	.....AGAATCTCTC CTTTCTCCTG CTTG.....	.....CTGA TCTGTCAACC TCCCAGGCAC.....
IFN A8	.....AGAATCTCTC CTTTCTCCTG CCTG.....	.....CTGA TCTGTCAACC TCCCAaGCAC.....

IFN A2 specific primer pair

IFN A1	....GaAGtATCTG CAAtATCTAC GATG.....	....GGGT GAGAGTCTTT GAAATGaCAG.....
IFN A2	....GCAGCATCTG CAACATCTAC AATG.....	....AAAC ATGAGTCTTT GAAATGGCAG.....
IFN A4	....GCAatATtTG CAACAT-ccC AATG.....	....AAGT --GAGTCTTT GAAATGGaAG.....
IFN A5	....GaAGCATCTG CAACcTCccC AATG.....	....AAAT --tAaTaTTT GAAAcGGCAG.....
IFN A6	....aCAGCATCTG CAACATCTAC AATG.....	....AAAC AAGAGTCTTT aAAATGGCAG.....
IFN A7	.... GtgatATtTG CAAaAT-ccC AATG.....	....AAGT --GAGTCTTT GAAATGGaAG.....
IFN A8	....GCAGCATCcG CAACATCTAC AATG.....	....AAAC AAGgGTCTTT GAAAgaGCAc.....

FIG. 5. General and *IFNA2*-specific primer sequences present in various human *IFNA* genes (25). The underlined sequences were used for PCR amplification. Lowercase letters indicate nucleotides distinct from those in the corresponding region of the primer. The 5′ and 3′ conserved primers correspond to nt +1067 to 1086 and nt +1415 to 1435, respectively. The *IFNA2*-specific primers correspond to nt +911 to 930 (5′) and nt +1565 to 1582 (3′).

Sendai virus- and imiquimod-induced cDNAs could also be restricted with *Hpa*I, suggesting the presence of *IFNA2* mRNA in induced cells (data not shown).

The amplified fragments were then cloned, and 25 transformants were selected for sequencing. As shown in Table 3, all the colonies amplified from the cDNA of Sendai virus-induced cells were identified as *IFNA8*, while the clones of amplified cDNA from imiquimod-induced cells consisted of *IFNA8* and *IFNA5*. The relative proportions of *IFNA8* and *IFNA5* were 77 and 23%, respectively. The preferential cloning of the *IFNA8* subtype may be due to the 100% homology of the selected primers with the *IFNA8* cDNA. Although the general primer pair was designed to recognize highly conserved regions of the *IFNA* genes, there were small differences in the sequences corresponding to the primer regions in *IFNA1*, *IFNA2*, *IFNA6*, *IFNA5*, and *IFNA4* cDNAs (Fig. 5). The conserved 5′-end primer selected shows 100% homology with the *IFNA8*, *IFNA7*, and *IFNA5* coding region, while all other corresponding coding regions show a single nucleotide difference. The 3′ primers selected show 100% homology with all the *IFNA* genes except *IFNA5* and *IFNA8*, which show a single nucleotide difference.

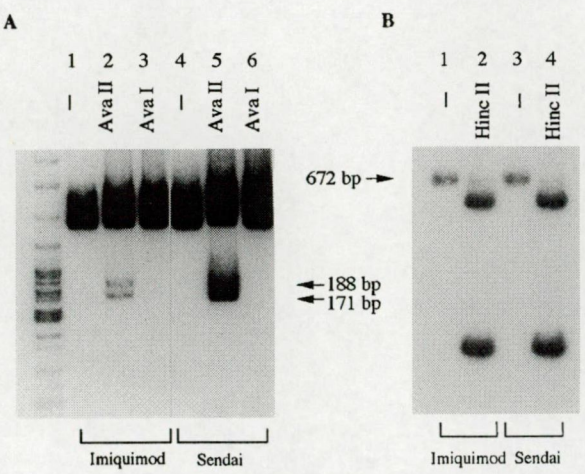

FIG. 6. Restriction analysis of DNA fragments amplified with a general and an *IFNA2*-specific set of primers. The RT-PCR was done as described in Materials and Methods with the end-labelled general and *IFNA2*-specific primers. General primers (A) amplified a 369-bp DNA fragment from imiquimod-induced (lanes 1 to 3) and Sendai virus-induced (lanes 4 to 6) cDNAs. Lanes 1 and 4 represent the uncut fragments; restriction with *Ava*II and the appearance of two fragments of 171 and 188 bp are shown in lanes 2 and 5. Lanes 3 and 6 show a lack of restriction with *Ava*I. The *IFNA2*-specific primer (B) amplified a 672-nt DNA fragment (lanes 1 and 3) that was restricted with *Hinc*II (lanes 2 and 4). Lanes 1 and 2 show amplification of a fragment from imiquimod-induced cDNAs, and lanes 3 and 4 show amplification of a fragment from Sendai virus-induced cDNAs. The amplified 672-bp fragment and the 171- and 188-bp fragments are marked.

Although a restriction analysis (with *Hph*I) of the amplified fragment suggested that *IFNA2* mRNA is present in both the imiquimod- and Sendai virus-induced cells, the *IFNA2* clone was not detected by sequencing. Therefore, we used a second *IFNA2*-specific primer pair (Fig. 5) to verify unequivocally the presence of this subtype. After amplification of cDNA from imiquimod- and Sendai virus-induced mRNAs, we obtained, as expected, the 672-bp fragment, which was restricted with *Hinc*II into 550- and 122-nt fragments (Fig. 6B). The presence of the *Hinc*II site in the amplified region is unique to *IFNA2*.

This 672-nt fragment was then cloned, and 50 colonies were selected and analyzed by restriction with *Hinc*II restriction endonuclease; all clones but one could be restricted with *Hinc*II and thus were identified as *IFNA2*. The undigested clone was identified as *IFNA6* by sequencing. All the clones obtained by cloning of an amplified fragment from Sendai virus-induced cells were characterized as *IFNA2* cDNA by *Hinc*II digestion. The reliability of the analysis with *Hinc*II was verified by se-

TABLE 3. *IFNA* subtypes expressed in imiquimod- and Sendai virus-stimulated PBMC

Stimulation	Result[a] for:								
	IFNA1	*IFNA13*	*IFNA2*	*IFNA4*	*IFNA5*	*IFNA6*	*IFNA7*	*IFNA8*	*IFNA14*
Sendai virus	+[b]	—	+[b,c]	—	—	—	—	+[d]	—
Imiquimod	+[b]	—	+[b,c]	—	+[d]	+[c]	—	+[d]	—

[a] —, not detected; +, present.
[b] Determined by restriction analysis of the IFN cDNA amplified by using general primers.
[c] Determined by restriction analysis and cloning of the IFN cDNA amplified with *IFNA2*-specific primers.
[d] Determined by cloning and sequencing of the IFN cDNA amplified with general primers.

quencing; sequences of two clones derived from imiquimod- and Sendai virus-induced samples were identical to *IFNA2*. Restriction analysis (Fig. 6B) indicated that a small portion of the 693-bp fragment was resistant to *Hin*cII restriction. This unrestricted fragment was isolated and cloned. The sequence analysis showed that this fragment represented *IFNA6* in imiquimod-induced cells, while it was identical to *IFNA2* in Sendai virus-infected cells. Thus, in summary, this analysis indicates that whereas imiquimod induces expression of *IFNA1*, *IFNA2*, *IFNA5*, *IFNA6*, and *IFNA8* in PBMC, in the same cells Sendai virus infection stimulates expression of *IFNA1*, *IFNA2*, and *IFNA8* (Table 3).

Induction of NF-κB-specific binding activity. Since the promoter regions of all the cytokine genes induced by imiquimod (except for *IFNA* genes) contain an NF-κB binding site, which plays a critical role in the inducible expression of these genes, we examined binding of nuclear proteins from imiquimod-induced cells and controls to DNA probes corresponding to the NF-κB sequences present in the HIV-1 LTR (78). Binding of nuclear proteins from CHX-treated cells and Sendai virus-infected cells was used as a positive control since both CHX and virus infection stimulate binding of the p50-p65 complex (16, 69, 76). Relatively high levels of constitutive nuclear NF-κB activity were observed in uninduced PBMC, since NF-κB is constitutively nuclear in mature B cells (54, 69). We therefore analyzed induced NF-κB binding in separated primary monocytes. Figure 7 shows the transient increase in the relative levels of NF-κB-specific complexes (A and B) that could be detected as early as 25 min after imiquimod induction, followed by a rapid decrease to basal levels. The formation of complex A was specific and could be completely inhibited by a 10-fold excess of the unlabelled probe (Fig. 7), while formation of complex B was slightly inhibited only by a 50-fold excess of unlabelled probe. In contrast, treatment with CHX induced a complex with mobility slightly faster than that of complex A. These data show that imiquimod treatment, similar to viral infection (16, 76), activates NF-κB-specific binding. Using antibodies specific to p50, p65, and c-rel, we have demonstrated, by mobility shift assay, the presence of p50 and c-rel but not p65 in the imiquimod-induced κB complexes (Fig. 7B).

Induction of α4F1-specific binding activity. The A4F1 element plays a critical role in the induction of murine *IFNA* genes (1), and the transcriptional activation of murine *IFNA* genes in virus-infected cells is associated with formation of a novel complex, A4F1/B (1, 2). Since the consensus of A4F1 sequence is also present in the inducible region (VRE) of human *IFNA* genes (Fig. 8C), we examined the binding of nuclear proteins from imiquimod-treated and virus-infected cells to DNA probes corresponding to the A4F1 sequence.

In the gel retardation assay, the binding of nuclear proteins from untreated cells shows the presence of a strong, slowly moving complex (complex A) and weak, fast-moving complexes (complexes B and C) (Fig. 8A, lane 1). In nuclear extracts from Sendai virus-infected cells or imiquimod-treated cells, a significant enhancement of complex B formation was detected (Fig. 8A, lanes 2, 3, 6, and 7). The formation of this complex was transient: enhancement was detected as early as 30 min after virus infection or imiquimod treatment (data not shown), and the levels of the A4F1/B complex returned to basic levels at 3 to 4 h postinduction. The formation of the A4F1/B complex was specific; it could be inhibited either with the unlabelled A4F1 probe or with the 35-nt-long inducible element (A4IE) of the *IFNA4* promoter region that contains the A4F1 sequence (Fig. 8B) but not with a nonspecific DNA such as pGEM plasmid or NF-κB probe (data not shown). The unlabelled A4F1 fragment also inhibited the formation of complex C, present in both the induced and uninduced nuclear proteins, but not complex A. In contrast, unlabelled A4IE effectively inhibited the formation of all complexes (A, B, and C). These results suggest that, similar to what occurs with murine cells (2), the formation of complex B is related to transcriptional activation of *IFNA* genes and that a similar complex(es) is induced in Sendai virus-infected and imiquimod-treated cells. However, it is unlikely that complex B

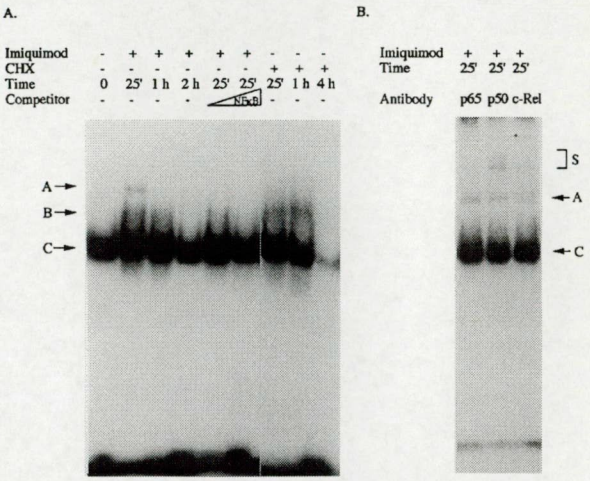

FIG. 7. Induction of NF-κB binding activities in imiquimod-induced monocytes. Monocytes were prepared from the adherent fraction of PBMC. Nuclear extracts were prepared as described in Materials and Methods from imiquimod-treated (3 μg/ml) cells at different times postinduction and analyzed for the presence of NF-κB activity by using oligonucleotides corresponding to the HIV-1 LTR NF-κB site (see Materials and Methods). All reaction mixtures contained 1 μg of a nonspecific competitor, poly(dI) · poly(dC). (A) The unlabelled probe was used as a specific competitor at 5- and 50-fold molar excesses. CHX-treated and uninduced cells were used as controls. (B) A supershift experiment with the indicated antibodies was done as described in Materials and Methods. +, present; −, absent; S, supershift.

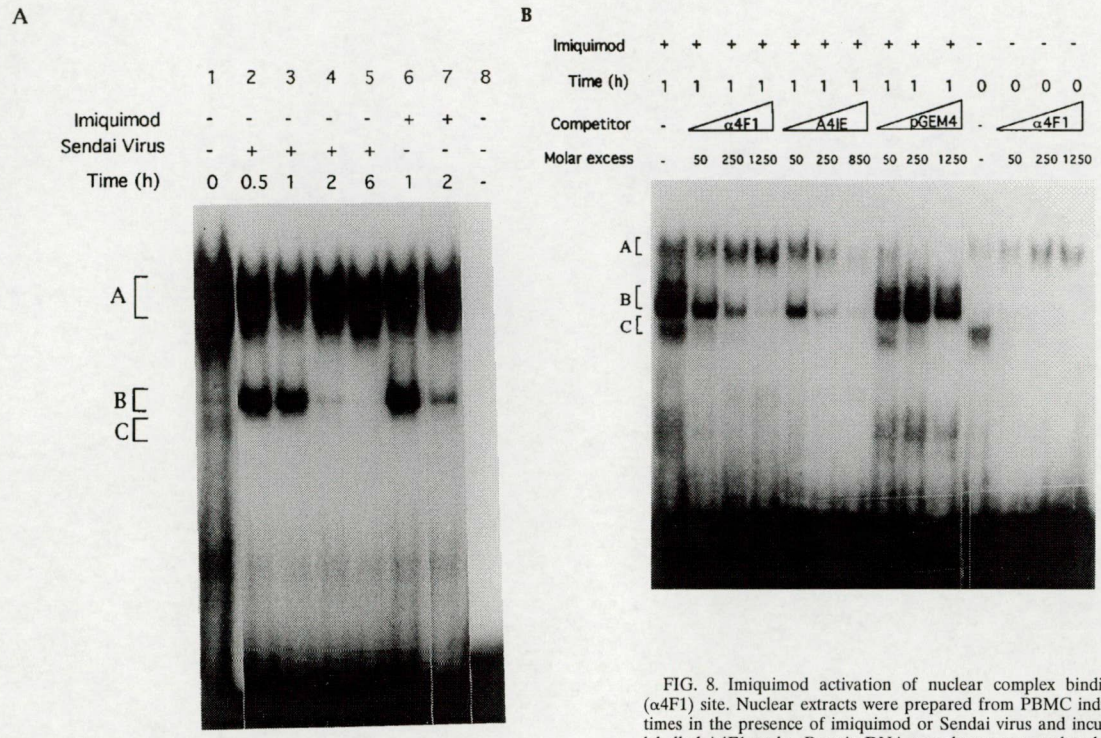

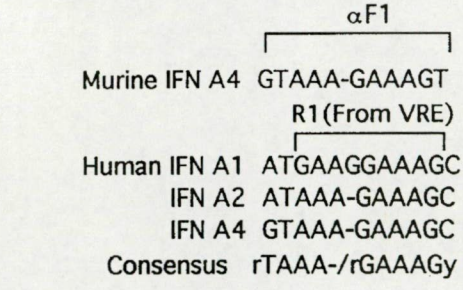

FIG. 8. Imiquimod activation of nuclear complex binding to the A4F1 (α4F1) site. Nuclear extracts were prepared from PBMC induced for different times in the presence of imiquimod or Sendai virus and incubated with a ^{32}P-labelled A4F1 probe. Protein-DNA complexes were analyzed on a nondenaturing gel as described in Materials and Methods. (A) Kinetics of formation of induction-specific A4F1 protein complex (A4F1/B). Lane 8 shows mobility of the probe alone, and lane 1 represents the complexes formed with extracts from the untreated cells. (B) Inhibition of A4F1/B complex formation. The ^{32}P-labelled A4F1 probe was preincubated for 15 min with nuclear extracts isolated from cells treated with imiquimod for 1 h, and then the indicated competitors were added in various molar excesses. α4F1 and A4IE represent the A4F1 sequence and VRE present in the murine *IFNA4* gene promoter region (2), and pGEM4 plasmid was used as a nonspecific DNA competitor. (C) Comparison of A4F1 binding sites in the VREs of murine and human *IFNA* promoters. r, purine residue; y, pyrimidine residue; +, present; −, absent.

represents binding of IRF-1 or NF-κB-specific proteins, since it could be supershifted neither with IRF-1-, p50-, p65-, nor c-rel-specific antibodies (data not shown).

Characterization of proteins binding to A4F1 by UV cross-linking. We have previously shown (2) that, in murine cells induced with virus, the A4F1/B complex contains at least two DNA-binding proteins, p96 and p68, but not the IRF-1 protein. To analyze the proteins binding to the A4F1 probe in Sendai virus-infected and imiquimod-treated PBMC, nuclear extracts prepared from Sendai virus-infected or imiquimod-treated cells at 1 h posttreatment were incubated with the BrdUrd-substituted A4IE probe. We used this probe rather than the A4F1 probe because the BrdUrd substitution in A4F1 altered the mobility of A4F1/B and A4F1/C complexes. The DNA-protein complexes were separated on nondenaturing gels (Fig. 9A) and UV cross-linked in situ, and the three complexes detected were individually eluted and subsequently analyzed by SDS-polyacrylamide gel electrophoresis (Fig. 9B).

While in uninduced cells we detected predominantly complex C, nuclear extracts from both Sendai virus-infected and imiquimod-induced cells showed a significant enhancement in formation of complexes A and B (Fig. 9A). Both of these complexes were efficiently inhibited with unlabelled A4IE oligonucleotides (data not shown). Cross-linking of the A4IE/A complex shows the presence of two DNA-protein adducts of 96 and 45 kDa present in both induced and uninduced cells (Fig. 7B). However, the A4IE/A complex from uninduced cells shows an additional DNA-protein adduct of about 55 kDa that is absent in induced cells. The A4IE/B complex shows the presence of 29- and 25-kDa DNA-protein adducts in both induced and uninduced cells (Fig. 9B). The fast-moving complex, A4IE/C, contains three DNA-protein adducts of 45, 29, and 25 kDa in induced cells, while in uninduced cells, only 29- and 25-kDa adducts were detected. The 28- and 25-kDa proteins are present in both induced and uninduced cells; however, the levels of the 29-kDa DNA-protein adduct detected in induced cells were much higher than those in uninduced cells, indicating that induction increased DNA binding of the 29-kDa protein. Thus, these data show that induction by Sendai virus or imiquimod results in (i) disappearance of binding of the 55-kDa protein to A4IE and (ii) increased binding of a 29-kDa protein. To determine whether the p55 and p29

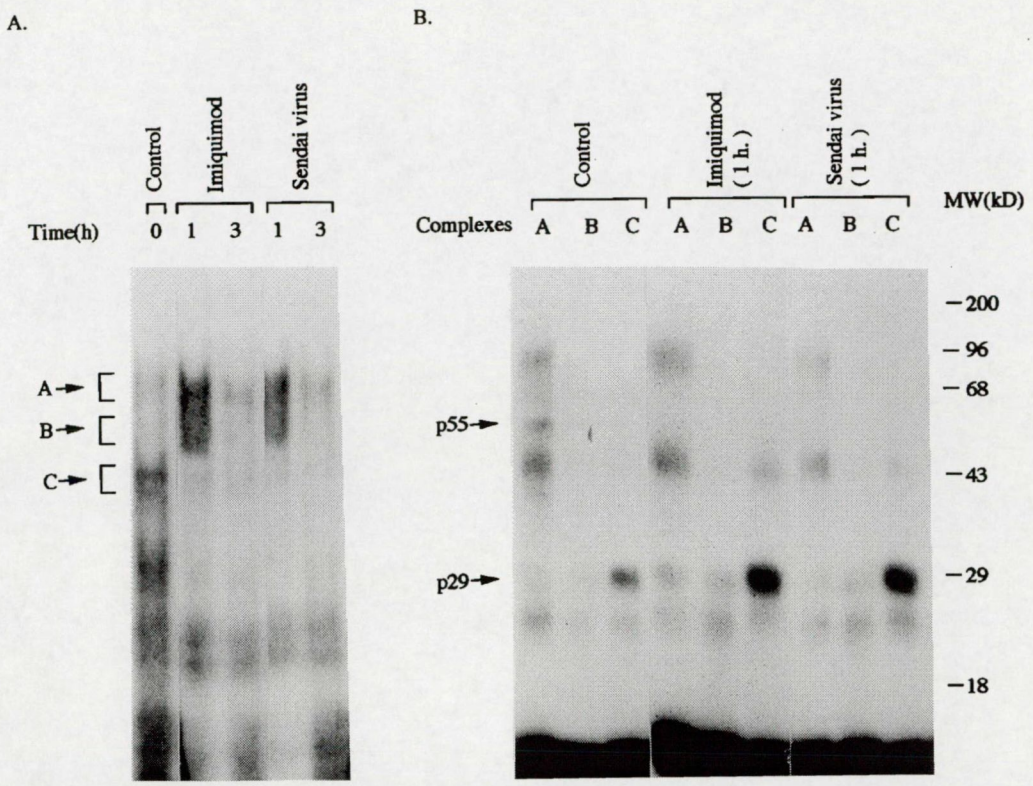

FIG. 9. UV cross-linking analysis of DNA-protein adduct formed between the IE sequence and nuclear extracts from imiquimod-treated and Sendai virus-infected cells. (A) Nuclear extracts prepared from induced cells at 1 and 3 h postinduction and from uninduced controls were incubated with the BrdUrd-substituted A4IE probe and resolved on a 4% acrylamide gel. (B) DNA and proteins were UV cross-linked in situ; gels were UV irradiated as described previously (78); bands corresponding to the A, B, and C complexes were eluted; and protein-DNA complexes were analyzed on an SDS–10% polyacrylamide gel. The molecular mass (MW) markers and the p55 and p29 DNA-protein adducts are indicated.

present in the uninduced cells represent IRF-2 and its proteolytic product (8, 57), we used the IRF-2 antibodies to analyze the presence of IRF-2 in the A4IE complexes. However, the IRF-2 antibodies did not supershift any of the A4IE complexes, nor did preabsorption of the extracts with these antibodies remove the p55 or p29 DNA-protein adduct (data not shown).

Imiquimod does not stimulate the appearance of new PRDI binding complexes. Virus-mediated induction of IFN genes has been associated with the induction of binding IRF-1 to PRDI. The same region can also bind IRF-2, which can repress IRF-1 activity (22). Induction-specific complexes PRDI-BFi and TH3 have been shown to contain cleaved IRF-2 or a 14-kDa N-terminal fragment of IRF-2 (8, 57). To determine whether imiquimod induces PRDI-specific binding, nuclear extracts from uninduced and imiquimod-induced cells were incubated with PRDI probe and DNA-protein complexes formed were analyzed by a gel retardation assay. Two DNA-protein complexes (A and B) were detected with extracts from uninduced cells (Fig. 10). These complexes were also observed after treatment with imiquimod; however, a small, transient increase in complex A formation was observed at the early stages of induction. The binding of complex A was easily inhibited by the unlabelled PRDI, while the decrease in binding of complex B required at least a 50-fold excess of the unlabelled probe. The unlabelled NF-κB probe did not complete the formation of these two complexes when used in a 5-fold excess, while a 50-fold excess decreased binding of both of these complexes. These results indicate the PRDI-specific binding of complex A. The identities of the proteins present in these complexes were examined by testing the abilities of various antibodies to modulate their formation. However, antiserum to neither IRF-1 nor IRF-2 could abolish formation of complex A or B (when added before formation of the complexes) or supershift these complexes (when added after complex formation) (data not shown). Since these antibodies were shown to interact with IRF-1 and IRF-2 on Western blot (immunoblot) analysis and by a supershift assay (27a), these data suggest that complexes A and B do not contain either IRF-1 or IRF-2.

DISCUSSION

We have shown in this study that imiquimod induces in PBMC expression of *IFNA/B* genes and cytokine genes, including IL-6, IL-8, and TNF-α genes. In contrast to viral infection, which effectively induces IFN genes in a large variety of primary cells and established cell lines, imiquimod was able to induce these genes only in primary human monocytes or in mouse spleen cells, and not in established lines of fibroblasts, B cells, or monocytes. Moreover, occasionally some PBMC did not respond to imiquimod stimulation and no IFN synthesis could be detected. The reasons for this unresponsiveness are presently unknown.

Induction of IFN and cytokine genes by imiquimod is transient and does not require cellular protein synthesis, indicating

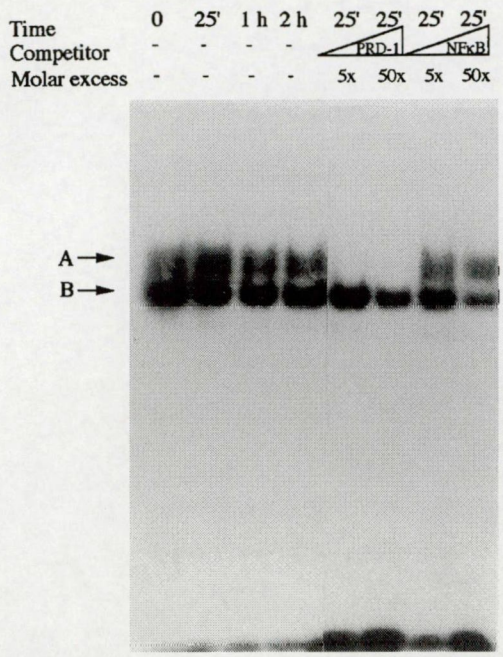

FIG. 10. Imiquimod does not stimulate PRDI-specific binding activity. Nuclear extracts prepared from imiquimod-induced cells and uninduced controls were incubated with ^{32}P-labelled PRDI probe, and the DNA-protein complexes were analyzed by a gel shift assay. Competition for complex formation was done with the unlabelled PRDI and NF-κB probes at 5- and 50-fold excesses.

that imiquimod, similar to viral infection, modifies or activates preexisting latent cellular factors. The fact that induction of *IFNA* and *IFNB* genes by these two inducers requires TK and PKC activity further emphasizes the importance of protein phosphorylation in the induction of these genes. The fact that virus and imiquimod induce similar sets of cytokine genes indicates that activation may involve a common *cis* element(s) conserved in the promoter regions of all these cytokine genes, such as an NF-κB binding site preserved in the promoter regions of all genes examined, except the *IFNA* genes. Stimulated transcription of the TNF-α gene was shown to involve interaction between NF-κB and AP-1 binding proteins, and transcription of IL-6 and IL-8 genes required interaction synergism between NF-IL6 and NF-κB (38, 44, 52); transcriptional activation of the *IFNB* gene depends on interaction between IRF-1, ATF-2, HMGI(Y), and the NF-κB complex (10, 75). Our data showed enhancement of NF-κB-specific binding in imiquimod-treated primary monocytes and suggest that NF-κB-specific binding may be required for the imiquimod-mediated activation of *IFNB*, TNF-α, IL-6, and IL-8 genes. Interestingly, imiquimod induced expression of the IL-8 gene more efficiently than did viral infection. It was recently shown that the NF-κB-like site in the IL-8 promoter region is activated by the c-rel/p65 complex (38), suggesting that the NF-κB-specific proteins induced by Sendai virus and imiquimod in PBMC may not be identical. Indeed, we have shown in this study the presence of p50 and c-rel in the imiquimod-induced NF-κB complexes, while virus infection was shown to predominantly activate the binding of the p50-p65 complex (76).

To analyze further the effect of imiquimod stimulation on the expression of *IFNA* genes, we identified the individual *IFNA* genes expressed in imiquimod-stimulated PBMC and compared them with Sendai virus-induced *IFNA* genes in these cells. It was previously shown (18, 29) that *IFNA1* and *IFNA2* are the major mRNAs present in virus-induced leukocytes, while *IFNA8*, *IFNA4*, *IFNA5*, *IFNA7*, *IFNA14*, *IFNA21*, and *IFNA16* mRNAs were identified as minor components. By PCR amplification and cloning, we detected *IFNA1*, *IFNA2*, and *IFNA8* in Sendai virus-induced human leukocytes. Under the same experimental conditions, *IFNA1*, *IFNA2*, *IFNA8*, *IFNA5*, and *IFNA6* were detected in imiquimod-induced PBMC. Although we cannot completely eliminate the possibility that another minor *IFNA* mRNA is present either in Sendai virus- or imiquimod-induced cells, these results indicate a higher degree of *IFNA* mRNA subtype heterogenicity in imiquimod-induced PBMC than in Sendai virus-infected cells.

The region (VRE) required for maximal inducibility of the human *IFNA1* and *IFNB* genes contains sets of GAAAGT and GAAATG repeats (14, 47, 48) that are also preserved in the inducible region of the murine *IFNA* gene promoters (58). When multimerized, these repeats serve as the binding site for IRF-1 and IRF-2 (22, 47), and IRF-1 was shown to activate these sequences in the yeast system (67) as well as in a transient expression assay (1). Nevertheless, our analysis did not show a significant increase in IRF-1-specific binding in imiquimod-treated PBMC. A virus-inducible, 35-nt sequence identified in a promoter of the murine *IFNA4* gene contains a symmetric sequence, GTAAAGAAAGT (A4F1), essential for the induction of the *IFNA4* promoter (2), that partially overlaps the putative IRF-1 binding site. This sequence is well preserved in the inducible region of murine and human *IFNA* genes, including those induced by imiquimod (Fig. 8C). In this study, we have shown that induction of *IFNA* genes in virus-infected and imiquimod-treated cells is associated with an induction-specific complex (A4F1/B) formed between the A4F1 sequence and nuclear extract from induced cells. The mobility of this complex could not be supershifted with either anti-IRF-1 or anti-IRF-2 antibodies or anti-STAT p91 antibodies (data not shown). The UV cross-linking analysis showed that at least four nuclear proteins bind to the 35-nt VRE. While the majority of DNA-protein adducts were identified in both induced and uninduced cells, two major differences in the binding profiles were observed. First, extracts from the control cells, but not from induced cells, show the presence of a 55-kDa protein that corresponds in size to the proteins of the IRF-1 family. The down-regulation of expression of *IFNA* and *IFNB* promoter regions by IRF-2 has been well documented in cotransfection experiments. Although the binding of IRF-2 to the inducible element could contribute to the negative regulation of this promoter (22, 23), we have not detected the presence of IRF-2 in the AF-1 complexes. Another PRDI zinc family binding protein has been shown to function as a repressor in cotransfection experiments (80); however, this protein is 88 kDa and therefore differs from the 55-kDa protein identified in the present study. The second difference is the increase in the relative levels of the 28-kDa DNA-protein adduct in induced cells, suggesting an increase in binding capacity or a more efficient cross-linking of the 28-kDa protein in induced cells. The possibility that this protein represents a processed form of IRF-2 (8, 57) cannot be eliminated, since the antibodies against IRF-2 used do not recognize the N-terminal region of this protein. These results, however, indicate that, similar to what has been observed with the murine system (2), the formation of an induction-specific complex B is not the result of binding of a novel protein to the inducible region but rather is the result of posttranslational modifications of the constitutively expressed binding proteins or their interaction with another non-DNA-binding component of the transcriptional

complex. Since the formation of the A4F1/B complex is abolished in the presence of TK and PKC inhibitors (data not shown), we suggest that imiquimod-induced phosphorylation of the preexisting A4F1 binding proteins is an essential step in the induction process.

The similarity between Sendai virus- and imiquimod-induced expression of IFN and cytokine genes may come as a major surprise to researchers in the IFN field. The requirement for dsRNA has been extensively documented for infections with a large variety of viruses (50). The present data suggest that activation by both these inducers involves phosphorylation rather than the presence of dsRNA per se. Phosphorylation was shown to play a role both in the dissociation or degradation of IκB complexes, leading to translocation of the NF-κB1 complex to the nucleus (5, 17), and in the activation of IRF-1 (79).

Recently, it has been shown that IFNs activate tyrosine kinases of the Jak family (9). These kinases directly phosphorylate proteins Stat91 and Stat113, which are part of the ISGF-3 complex that binds to the IFN-responsive element (ISRE) of the IFN-activated genes and activates transcription of these genes (31, 66). We have shown (63) that a priming with IFN (73) enhances virus-induced expression of IFN-α/β, as well as the other cytokines, e.g., IL-6 and TNF-α. Accordingly, priming with IFN enhanced imiquimod-stimulated expression of *IFNA* and *IFNB* genes (data not shown). It is likely, therefore, that IFN provides a costimulation signal both in the imiquimod- and virus-induced phosphorylation pathways. Activation of a signal transduction by a synthetic ligand able to aggregate membrane receptors was used to study the T-cell receptor-mediated signalling pathway (72). The membrane-permeable imiquimod may, therefore, function as a ligand, alter intramembrane interactions, and initiate intracellular signalling. Furthermore, the direct binding of pyridinyl-imidazole compounds to mitogen-activated protein kinase (CSBP) with a consequent inhibition of kinase activity reported recently (41) raises the possibility that imiquimod interacts directly with a kinase modulating the transduction pathway leading to the transcriptional activation of the cytokine genes.

The fact that imiquimod inhibits virus-mediated induction of *IFNA* genes while it superinduces induction of *IFNB* and IL-6 genes indicates that induction of *IFNA* may proceed by a pathway distinct from that for the other cytokines examined and adds to the complexity of both the pleiotropic effects of these inducers and the mechanisms by which these genes are activated. Finally, the use of imiquimod and its analogs may provide a useful tool for dissecting the role of kinase pathways in the virus-mediated signal transduction inducing inflammatory cytokines.

ACKNOWLEDGMENTS

We thank Jean Content, Tadatsugu Taniguchi, Bruce Beutler, and Jan Vilček for the IL-6, IRF-1, TNF-α, and IL-8 probes; John Hiscott and Nancy Rice for the gift of IRF-1, IRF-2, p50, p65, and c-rel antibodies; and Pamela Talalay for her critical comments on the manuscript.

This study was supported by a grant from 3M Pharmaceuticals and by grant AI26123 from the National Institutes of Health (NIAID).

REFERENCES

1. Au, W.-C., N. B. K. Raj, R. Pine, and P. M. Pitha. 1992. Distinct activation of murine interferon-α promoter region by IRF-1/ISFG-2 and virus infection. Nucleic Acids Res. 20:2877–2884.
2. Au, W.-C., Y. Su, N. B. K. Raj, and P. M. Pitha. 1993. Virus-mediated induction of IFNA gene requires cooperation between multiple binding factors in the IFNA promoter region. J. Biol. Chem. 268:24032–24040.
3. Bisat, F., N. B. K. Raj, and P. M. Pitha. 1988. Differential and cell type specific expression of murine alpha-interferon genes is regulated on the transcriptional level. Nucleic Acids Res. 16:6067–6083.
4. Boyum, A. 1968. Isolation of mononuclear cells and granulocytes from human cells. Scand. J. Clin. Lab. Invest. 21(Suppl. 97):1–72.
5. Brown, K., S. Park, T. Kanno, G. Franzoso, and U. Siebenlist. 1993. Mutual regulation of the transcriptional activator NF-κB and its inhibitor, Iκα. Proc. Natl. Acad. Sci. USA 90:2532–2536.
6. Chen, M., B. P. Griffith, H. L. Lucia, and G. D. Hsiung. 1988. Efficacy of S26308 against guinea pig cytomegalovirus infection. Antimicrob. Agents Chemother. 32:678–683.
7. Chirgwin, J. M., A. E. Przybyla, R. J. MacDonald, and W. J. Rutter. 1979. Isolation of biologically active ribonucleic acid from sources enriched in ribonuclease. Biochemistry 18:5294–5299.
8. Cohen, L., and J. Hiscott. 1992. Characterization of TH3, an induction-specific protein interacting with the interferon β promoter. Virology 191: 589–599.
9. Darnell, J. E., I. M. Kerr, and G. R. Stark. 1994. Jak-Stat pathways and transcriptional activation in response to IFNs and other extracellular signalling proteins. Science 264:1415–1421.
9a. Diaz, M. O., S. Bohlander, and G. Allen. 1993. Nomenclature of human interferon genes. J. Interferon Res. 13:443–444.
10. Du, W., D. Thanos, and T. Maniatis. 1993. Mechanism of transcriptional synergism between distinct virus inducible enhancer elements. Cell 74:887–878.
11. Field, A. K., A. A. Tytell, G. P. Lampson, and E. M. Hilleman. 1967. Inducers of interferon and host resistance. II. Multistranded synthetic polynucleotide complexes. Proc. Natl. Acad. Sci. USA 58:1004–1010.
12. Fitzgerald-Bocarsly, P., D. M. Howell, L. Pettera, S. Tehrani, and C. Lopez. 1991. Immediate-early gene expression is sufficient for induction of natural killer cell-mediated lysis of herpes simplex virus type 1-infected fibroblasts. J. Virol. 65:3151–3160.
13. Fondal, M. 1976. SRBC rosette formation as a human T lymphocyte marker. Scand. J. Immunol. 5:69–76.
14. Fujita, T., S. Ohno, H. Yasumitsu, and T. Taniguchi. 1985. Delimitation and properties of DNA sequences required for the regulated expression of human interferon-β gene. Cell 41:489–496.
15. Fujita, T., L. F. L. Reis, N. Watanabe, Y. Kimura, T. Taniguchi, and J. Vilcek. 1989. Induction of the transcription factor IRF-1 and interferon-β mRNAs by cytokines and activators of second-messenger pathways. Proc. Natl. Acad. Sci. USA 86:9936–9940.
16. Garoufalis, E., I. Kwan, R. Lin, A. Mustafa, N. Pepin, A. Roulston, J. Lacoste, and J. Hiscott. 1994. Viral induction of the human beta interferon promoter: modulation of transcription of NF-κB/*rel* proteins and interferon regulatory factors. J. Virol. 68:4707–4715.
17. Ghosh, S., and D. Baltimore. 1990. Activation *in vitro* of NF-κB by phosphorylation of its inhibitor IκB. Nature (London) 344:678–682.
18. Goeddel, D. V., D. W. Leung, T. J. Dull, M. Gross, R. M. Lawn, R. McCandliss, P. H. Seeburg, A. Ullrich, E. Yelverton, and P. W. Gray. 1981. The structure of eight distinct cloned human leukocyte interferon cDNAs. Nature (London) 290:20–26.
19. Goodbourn, S., H. Burstein, and T. Maniatis. 1986. The human β-interferon gene enhancer is under negative control. Cell 45:601–610.
20. Goodbourn, S., K. Zinn, and T. Maniatis. 1985. Human β-interferon gene expression is regulated by an inducible enhancer element. Cell 41:509–520.
21. Goren, T., A. Kapitkovsky, A. Kimchi, and M. Rubinstein. 1983. High and low potency interferon-alpha subtypes induce (2'-5') oligoadenylate synthetase with similar efficiency. Virology 130:273–280.
22. Harada, H., T. Fujita, M. Miyamoto, Y. Kimura, M. Maruyama, A. Furia, T. Miyata, and T. Taniguchi. 1989. Structurally similar but functionally distinct factors, IRF-1 and IRF-2, bind to the same regulatory elements of IFN and IFN-inducible genes. Cell 58:729–739.
23. Harada, H., K. Willison, J. Sakakibara, M. Miyamoto, T. Fujita, and T. Taniguchi. 1990. Absence of the type I IFN system in EC cells: transcriptional activator (IRF-1) and repressor (IRF-2) genes are developmentally regulated. Cell 63:303–312.
24. Harrison, C. J., L. Jenski, T. Voychehovski, and D. I. Bernstein. 1988. Modification of immunological responses and clinical disease during topical R-837 treatment of genital HSV-2 infection. Antiviral Res. 10:209–223.
25. Henco, K., J. Brosius, A. Fujisawa, J.-I. Fujisawa, J. R. Haynes, J. Hochstadt, T. Kovacic, M. Pasek, A. Schambock, J. Schmid, K. Todokoro, M. Walchli, S. Nagata, and C. Weissmann. 1985. Structural relationship of human interferon alpha genes and pseudogenes. J. Mol. Biol. 185:227–260.
26. Henderson, D. R., and W. K. Joklik. 1979. The mechanism of interferon induction by UV-irradiated reovirus. Virology 91:389–406.
27. Henkel, T., T. Machleidt, I. Alkalay, M. Kronke, Y. Ben-Neriah, and P. A. Baeuerle. 1993. Rapid proteolysis of IκBα is necessary for activation of transcription factor NF-κB. Nature (London) 365:182–185.
27a. Hiscott, J. Personal communication.
28. Hiscott, J., D. Alper, L. Cohen, J. F. Leblanc, L. Sportza, A. Wong, and S. Xanthoudakis. 1989. Induction of human interferon gene expression is associated with a nuclear factor that interacts with the NF-κB site of the human immunodeficiency virus enhancer. J. Virol. 63:2557–2566.

29. **Hiscott, J., K. Cantell, and C. Weissmann.** 1984. Differential expression of human interferon genes. Nucleic Acids Res. 12:3727–3746.
30. **Ho, M.** 1973. Animal viruses and interferon formation, p. 29–44. *In* N. B. Finter (ed.), Interferons and interferon inducers. Elsevier Publishers B.V., Amsterdam.
31. **Hunter, T.** 1993. Signal transduction. Cytokine connections. Nature (London) 366:114–116.
32. **Johnston, M. D., and D. C. Burke.** 1973. Interferon induction by virus: molecular requirements, p. 124–148. *In* W. E. Carter (ed.), Selective inhibitors of viral functions. CRC Press, New York.
33. **Joklik, W. K.** 1980. Induction of interferon by reovirus, p. 200–203. *In* D. Schlessinger (ed.), Microbiology—1980. American Society for Microbiology, Washington, D.C.
34. **Keller, A. D., and T. Maniatis.** 1991. Identification and characterization of a novel repressor of β-interferon gene expression. Genes Dev. 5:868–879.
35. **Kelley, K. A., and P. M. Pitha.** 1985. Characterization of a mouse interferon gene locus II. Differential expression of α-interferon genes. Nucleic Acids Res. 13:825–839.
36. **Kumagai, K., H. K. Ito, S. Hinuma, and M. Tada.** 1979. Pretreatment of plastic petri dishes with fetal calf serum. A simple method for macrophage isolation. J. Immunol. Methods 29:17–25.
37. **Kumar, A., S. J. Haque, J. Hiscott, and B. R. G. Williams.** 1992. The interferon induced p68 protein kinase regulates transcription factor NF-κB via phosphorylation of its inhibitor IκB. J. Interferon Res. 12:S207.
38. **Kunsch, C., and C. A. Rosen.** 1993. NF-κB subunit-specific regulation of the interleukin-8 promoter. Mol. Cell. Biol. 13:6137–6146.
39. **Langer, J. A., and S. Pestka.** 1988. Interferon receptors. Immunol. Today 9:393–400.
40. **Laude, H., J. Gelfi, L. Lavenant, and B. Charley.** 1992. Single amino acid changes in the viral glycoprotein M affect induction of alpha interferon by the coronavirus transmissible gastroenteritis virus. J. Virol. 66:743–749.
41. **Le, J. C., J. T. Laydon, P. C. McDonnell, T. F. Gallagher, S. Kumar, D. Green, D. McNulty, M. J. Blumenthal, J. R. Heys, S. W. Landvatter, J. E. Strickler, M. M. McLaughlin, I. R. Siements, S. M. Fisher, G. P. Livi, J. R. White, J. L. Adams, and P. R. Young.** 1994. A protein kinase involved in the regulation of inflammatory cytokine biosynthesis. Nature (London) 372:739–746.
42. **Lebon, P.** 1985. Inhibition of herpes simplex virus type 1-induced interferon synthesis by monoclonal antibodies against viral glycoprotein D and by lysosomotropic drugs. J. Gen. Virol. 66:2781–2786.
43. **Lenardo, M. J., C.-M. Fan, T. Maniatis, and D. Baltimore.** 1989. The involvement of NF-κB in β-interferon gene regulation reveals its role as widely inducible mediator of signal transduction. Cell 57:287–294.
44. **Libermann, T. A., and D. Baltimore.** 1990. Activation of interleukin-6 gene expression through the NF-κB transcription factor. Mol. Cell. Biol. 10:2327–2334.
45. **Lieberman, A. P., P. M. Pitha, H. S. Shin, and M. L. Shin.** 1989. Poly(A) removal is the kinase-regulated step in tumor necrosis factor mRNA decay. Proc. Natl. Acad. Sci. USA 86:6348–6352.
46. **Long, W. F., and D. C. Burke.** 1971. Interferon production by double-stranded RNA: a comparison of induction by reovirus to that by a synthetic double-stranded polynucleotide. J. Gen. Virol. 12:1–11.
47. **MacDonald, N. J., D. Kuhl, D. Maguire, D. Naf, P. Gallant, A. Goswamy, H. Hug, H. Bueler, M. Chaturvedi, J. de la Fuente, H. Ruffner, F. Meyer, and C. Weissmann.** 1990. Different pathways mediate virus inducibility of the human IFN-α1 and IFN-β genes. Cell 60:767–779.
48. **Maniatis, T., L.-A. Whittemore, W. Du, C.-M. Fan, A. D. Keller, V. Palombella, and D. Thanos.** 1992. Positive and negative regulation of the human interferon-β gene expression, p. 1193–1220. *In* S. L. McKnight and K. Yamamoto (ed.), Transcriptional regulation. Cold Spring Harbor Laboratory Press, Cold Spring Harbor, N.Y.
49. **Maran, A., R. K. Maitra, A. Kumar, B. Dong, W. Xiao, G. Li, B. R. G. Williams, P. F. Torrence, and R. H. Silverman.** 1994. Blockage of NF-κB signaling by selective ablation of an mRNA target by 2-5A antisense chimeras. Nature (London) 265:789–792.
50. **Marcus, P. I.** 1984. Interferon induction by viruses: double-stranded ribonucleic acid as the common proximal inducer molecule, p. 113–175. *In* R. M. Friedman (ed.), Interferons 3. Mechanisms of production and action. Elsevier Science Publishers B.V., Amsterdam.
51. **Marcus, P. I., and M. J. Sekellick.** 1977. Defective interfering particles with covalently linked [+] RNA induce interferon. Nature (London) 266:815–819.
52. **Matsusaka, T., K. Fujikawa, Y. Nishio, N. Mukaida, K. Matsushima, T. Kishimoto, and S. Akira.** 1993. Transcription factors NF-IL6 and NF-κB synergistically activate transcription of the inflammatory cytokines, interleukin 6 and interleukin 8. Proc. Natl. Acad. Sci. USA 90:10193–10197.
53. **Matsuyama, T., T. Kimura, M. Kitagawa, K. Pfeffer, T. Kawakami, N. Watanabe, T. M. Kundig, R. Amakawa, K. Kishihara, A. Wakeham, J. Potter, C. L. Furlonger, A. Narendran, H. Suzuki, P. S. Ohashi, C. J. Paige, T. Taniguchi, and T. W. Mak.** 1993. Targeted disruption of IRF-1 or IRF-2 results in abnormal type I IFN gene induction and aberrant lymphocyte development. Cell 75:83–97.
54. **Miyamoto, S., M. J. Schmitt, and I. M. Verma.** 1994. Qualitative changes in the subunit composition of κB-binding complexes during murine B-cell differentiation. Proc. Natl. Acad. Sci. USA 91:5056–5060.
55. **Mizoguchi, J., P. M. Pitha, and N. B. K. Raj.** 1985. Efficient expression in Escherichia coli of two species of human interferon-α and their hybrid molecules. DNA 4:221–232.
56. **Ortaldo, J. R., R. B. Herberman, C. Harvey, P. Osheroff, Y.-C. E. Pan, B. Kelder, and S. Pestka.** 1984. A species of human α-interferon that lacks the ability to boost human natural killer activity. Proc. Natl. Acad. Sci. USA 81:4926–4929.
57. **Palombella, V. J., and T. Maniatis.** 1992. Inducible processing of interferon regulatory factor-2. Mol. Cell. Biol. 12:3325–3336.
58. **Raj, N. B. K., W.-C. Au, and P. M. Pitha.** 1991. Identification of a novel virus-responsive sequence in the promoter of murine interferon-α genes. J. Biol. Chem. 266:11360–11365.
59. **Raj, N. B. K., M. Kellum, K. A. Kelley, S. Antrobus, and P. M. Pitha.** 1985. Differential regulation of interferon synthesis in lymphoblastoid cells. J. Interferon Res. 5:493–510.
60. **Raj, N. B. K., and P. M. Pitha.** 1981. Analysis of interferon messenger RNA in human fibroblast cells induced to produce interferon. Proc. Natl. Acad. Sci. USA 78:7426–7430.
61. **Raj, N. B. K., and P. M. Pitha.** 1983. Two levels of regulation of β-interferon gene expression in human cells. Proc. Natl. Acad. Sci. USA 80:3923–3927.
62. **Reis, L. F., H. Harada, J. D. Wolchok, T. Taniguchi, and J. Vilcek.** 1992. Critical role of a common transcription factor, IRF-1, in the regulation of IFN-β and IFN-inducible genes. EMBO J. 11:185–193.
63. **Rosztoczy, I., and P. M. Pitha.** 1993. Priming does not change promoter sequence requirements for IFN induction or correlate with the expression of IFN regulatory factor-1. J. Immunol. 151:1303–1311.
64. **Ruffner, H., L. F. Reis, D. Nef, and C. Weissmann.** 1993. Induction of type I interferon genes and interferon-inducible genes in embryonal stem cells devoid of interferon regulatory factor 1. Proc. Natl. Acad. Sci. USA 90:11503–11507.
65. **Ryals, J., P. Dierks, H. Ragg, and C. Weissmann.** 1985. A 46-nucleotide promoter segment from an IFN-α gene renders an unrelated promoter inducible by virus. Cell 41:495–507.
66. **Sadowski, H. B., K. Shuai, J. E. Darnell, Jr., and M. Z. Gilman.** 1993. A common nuclear signal transduction pathway activated by growth factor and cytokine receptors. Science 261:1739–1744.
67. **Sailer, A., K. Nagata, D. Naf, M. Aebi, and C. Weissmann.** 1992. Interferon regulatory factor-1 (IRF-1) activates the synthetic IRF-1-responsive sequence (GAAAGT)4 in Saccharomyces cerevisiae. Gene Expr. 2:329–337.
68. **Sanger, F., S. Nicklen, and A. R. Coulson.** 1977. DNA sequencing with chain-terminating inhibitors. Proc. Natl. Acad. Sci. USA 74:5463–5467.
69. **Sen, R., and D. Baltimore.** 1986. Inducibility of κ immunoglobulin enhancer-binding protein NF-κB by a posttranslational mechanism. Cell 47:921–928.
70. **Shuttleworth, J., J. Morser, and D. C. Burke.** 1983. Expression of interferon-α and interferon-β genes in human lymphoblastoid (Namalwa) cells. Eur. J. Biochem. 133:399–404.
71. **Sidky, Y. A., E. C. Borden, C. E. Weeks, M. J. Reiter, J. F. Hatcher, and G. T. Bryan.** 1992. Inhibition of murine tumor growth by an interferon-inducing imidazoquinolinamine. Cancer Res. 52:3528–3533.
72. **Spencer, D. M., T. J. Wandless, S. L. Schreiber, and G. R. Crabtree.** 1993. Controlling signal transduction with synthetic ligands. Science 262:1019–1024.
73. **Stewart, W. E., II, L. B. Gosser, and R. Z. Lockart.** 1971. Priming: a non-antiviral function of interferon. J. Virol. 7:792–801.
74. **Taira, H., T. Kanda, T. Omata, H. Shibuta, M. Kawakita, and K. Iwasaki.** 1987. Interferon induction by transfection of Sendai virus C gene cDNA. J. Virol. 61:625–628.
75. **Thanos, D., and T. Maniatis.** 1992. The high mobility group protein HMG I(Y) is required for NF-κB-dependent virus induction of the human IFN-β gene. Cell 71:777–789.
76. **Thanos, D., and T. Maniatis.** 1995. Identification of the rel family members required for virus induction of the human beta interferon gene. Mol. Cell. Biol. 15:152–164.
77. **Visvanathan, K. V., and S. Goodbourn.** 1989. Double-stranded RNA activates binding of NF-κB to an inducible element in the human β interferon promoter. EMBO J. 8:1129–1138.
78. **Vlach, J., and P. M. Pitha.** 1992. Herpes simplex virus type 1-mediated induction of human immunodeficiency virus type 1 provirus correlates with binding of nuclear proteins to the NF-κB enhancer and leader sequence. J. Virol. 66:3616–3623.
79. **Watanabe, N., J. Sakakibara, A. G. Hovanessian, T. Taniguchi, and T. Fujita.** 1991. Activation of IFN-β element by IRF-1 requires a posttranslational event in addition to IRF-1 synthesis. Nucleic Acids Res. 19:4421–4428.
80. **Whittemore, L.-A., and T. Maniatis.** 1990. Postinduction repression of the β-interferon gene is mediated through two positive regulatory domains. Proc. Natl. Acad. Sci. USA 87:7799–7803.
81. **Yasuda, Y., E. Ohgitani, A. Yamada, Y. Hosaka, K. Uno, J. Imanishi, and T. Kishida.** 1992. Induction of interferon-α in human peripheral blood mononuclear cells by influenza virus: role of viral glycoproteins. J. Interferon Res. 12(Suppl.):S141.

IV.

Virology 259, 74–84 (1999)
Article ID viro.1999.9757, available online at http://www.idealibrary.com on IDEAL®

Involvement of a p53-Dependent Pathway in Rubella Virus-Induced Apoptosis

Klara Megyeri,*,† Klara Berencsi,* Thanos D. Halazonetis,* George C. Prendergast,* Giorgia Gri,* Stanley A. Plotkin,‡ Giovanni Rovera,* and Eva Gönczöl*,†,[1]

*The Wistar Institute, 3601 Spruce Street, Philadelphia, Pennsylvania 19104; †Department of Microbiology, Albert Szent-Györgyi Medical University, Dom ter 10, Szeged, H-6720, Hungary; and ‡Pasteur Merieux Connaught, 4650 Wismer Road, Doylestown, Pennsylvania 18901

Received October 6, 1998; returned to author for revision December 8, 1998; accepted April 1, 1999

In light of the important role of apoptotic cell death in the pathogenesis of several viral infections, we asked whether the cytopathogenicity evoked by rubella virus (RV) might also involve apoptotic mechanisms. The To-336 strain of RV induced apoptosis in Vero and RK-13 cells, but not in fibroblast cell lines. UV-inactivated RV virions did not elicit the apoptotic response, indicating that productive infection is required for the induction of cell death. Both p53 and p21 protein levels were highly elevated in RV-infected Vero cells. The level of p21 mRNA was increased, while expression of the p53 gene was unaffected by RV infection. A dominant-negative p53 mutant ($p53^{W248}$) conferred partial protection from RV-induced apoptosis. These data implicate a p53-dependent apoptotic pathway in the cytopathogenicity of RV, thereby suggesting a mechanism by which RV exerts its teratogenic effects. © 1999 Academic Press

INTRODUCTION

Viruses rely on cellular metabolites and enzymes for their replication and perturb many strictly monitored biochemical processes. Viral infections may influence cell division by interfering with the function of cell cycle regulatory proteins or by altering cellular gene expression (reviewed in Jansen-Dürr, 1996). Such perturbations, in turn, frequently trigger apoptosis, a phylogenetically conserved self-destructive biological response that eliminates damaged cells. Thus apoptosis, as a part of the natural defense mechanism that protects against viral infections, plays an important role in the pathogenic mechanisms of many different viruses (reviewed in Razvi and Welsh, 1995). In the course of their replication cycles, adenovirus, Epstein-Barr virus, human papillomaviruses, and hepatitis B virus induce p53-dependent apoptosis (Lowe and Ruley, 1993; Allday *et al.*, 1995; Chen and Cooper, 1996; Chirillo *et al.*, 1997; Desaintes *et al.*, 1997). However, all of these viruses have also evolved complex strategies to inactivate the p53 protein or to counteract its biological action (Debbas and White, 1993; Subramanian *et al.*, 1993, 1995; Okan *et al.*, 1995; Gillet and Brun, 1996). Other viruses, including influenza viruses, human immunodeficiency virus, and human herpesvirus 6, may induce cell death through p53-independent mechanisms. For example, virally induced apoptosis was shown to be mediated by interferon-induced enzymes, including the interferon-induced double-stranded RNA-dependent protein kinase and the 2–5 Å synthetase/RNaseL, or by activation of the Fas and tumor necrosis factor-receptor signaling pathways (Wada *et al.*, 1995; Takizawa *et al.*, 1996; Diaz-Guerra *et al.*, 1997; Lee *et al.*, 1997; Su and Schneider, 1997). Some viruses encode proteases that cleave polyprotein precursor molecules synthesized during their replication. These viral proteases may also promote apoptosis when they bind their cellular substrates (Strack *et al.*, 1996).

Rubella virus (RV) is the sole member of the *Rubivirus* genus in the family Togaviridae, which also includes the *Alphavirus* genus. The ability of alphaviruses to elicit apoptosis is well-documented (Levine *et al.*, 1993; Griffin and Hardwick, 1997). The cytopathic effect (CPE) observed in cell cultures infected with the prototype alphavirus, Sindbis virus (SV), is known to be mediated by apoptosis (Levine *et al.*, 1993). The transmembrane domains of the SV envelope glycoproteins were shown to be essential for the induction of apoptosis (Joe *et al.*, 1998). The apoptotic pathway triggered by this virus involves the action of NF-κB (Lin *et al.*, 1995, 1998). Overexpression of bcl-2 inhibits SV-induced cell death, with an accompanying shift of the infectious cycle from a lytic to a persistent phase (Levine *et al.*, 1993). Furthermore, a clear example of how apoptotic cell death can represent the central mechanism of virulence came from studies identifying neuronal apoptosis as the underlying process that contributes to SV-induced encephalitis in susceptible mice (Levine *et al.*, 1996; Lewis *et al.*, 1996). RV is the causative agent of rubella or German measles. The clinical course of natural childhood rubella is usually mild and frequently asymptomatic, whereas establishment of persistent and generally noncytopathic RV infection of the fetus may cause profound damage in the ontogeny of

[1] To whom correspondence and reprint requests should be addressed. Fax: (215) 898-3868. E-mail: gonczol@wistar.upenn.edu.

0042-6822/99 $30.00

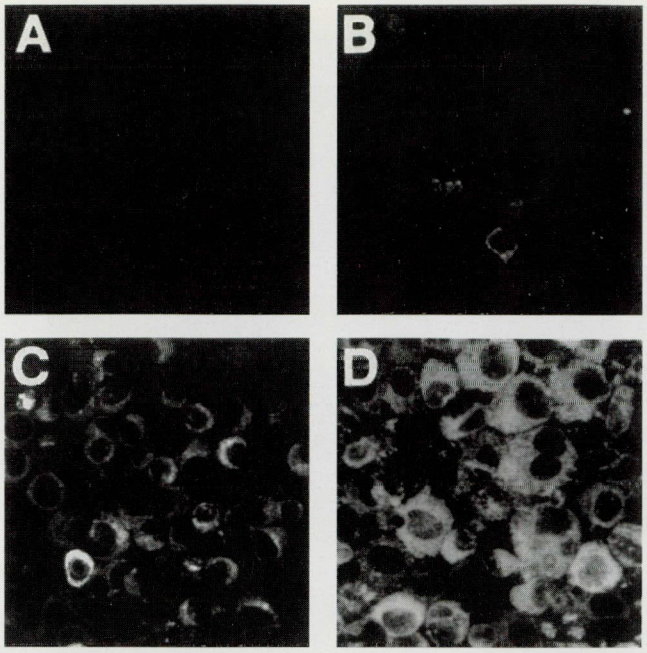

FIG. 1. Kinetics of RV replication in Vero cells. RV replication was examined by indirect immunofluorescence assay using RV envelope glycoprotein E1-specific MAb and FITC-conjugated goat anti-mouse immunoglobulin. Vero cells were infected with the To-336 strain of RV, incubated for 1, 3, and 5 days, stained, and visualized by confocal microscopy (B, C, and D, respectively). (A) Mock-infected cells cultured in parallel for 5 days.

fetal organs (reviewed in Wolinsky, 1996). Histological evidence of cell death, possibly due to a direct cytopathic effect of RV, can also be demonstrated in various organs (Bellanti *et al.,* 1965; Tondury and Smith, 1966; Singer *et al.,* 1967; Driscoll, 1969). The teratogenic effect of RV is manifested in the complex clinical signs of intrauterine growth retardation and organ-specific dysfunctions defined as congenital rubella syndrome (CRS) (reviewed Naeye and Blanc, 1965; Plotkin *et al.,* 1965a; Rawls and Melnick, 1966; Plotkin, 1994; Wolinsky, 1996). Comparative laboratory studies revealed that RV can establish persistent, noncytocidal infection in many cell types, while only a limited number of tissue culture systems, including kidney cell lines isolated from different animal species (Vero, RK-13, and BHK-21), human fetal lens cells, and a rabbit cornea cell line, were shown to be susceptible to the cytopathic effect of this virus (McCarthy, 1969; Wolinsky, 1996). Characteristic features of RV replication in cultured cells include slow, asynchronous infection, with a variable percentage of infectable cells depending on the cell type (Wolinsky, 1996). For virus isolation and for analyses of the mechanism of RV infection, the Vero cell line is most frequently used, because these cells efficiently support viral replication, exhibit extensive CPE, and show a high frequency of infection (~100% (Hemphill *et al.,* 1988). *In vitro* studies have demonstrated that RV infection slows the growth rate of human diploid fibroblasts, causes mitotic arrest, and ultimately gives rise to genetic alterations, such as chromosomal breaks (Plotkin *et al.,* 1965b; Nusbacher *et al.,* 1967). RV-induced synthesis of a mitotic inhibitor perturbs physiological cell cycle regulation and thus affects cell growth (Plotkin and Vaheri, 1967). RV infection also causes cytomorphological alterations in the membrane systems of the endoplasmic reticulum, Golgi complex, and mitochondria (Lee *et al.,* 1996), depolymerization of actin filaments (Bowden *et al.,* 1987), and an altered responsiveness to certain cytokines, such as epidermal growth factor (Yoneda *et al.,* 1986). It has long been suggested that the complex pathophysiological basis of CRS rests in the concerted action of altered cell growth, impaired differentiation, and death of certain sensitive cell types (Plotkin *et al.,* 1965a; Dudgeon, 1969; Wolinsky, 1996). However, the underlying mechanisms involved in the cytopathogenicity of RV have remained unclear.

In the present study, we investigated the molecular events implicated in RV-induced cell death in an effort to gain some insight into the teratogenic effect of this virus.

RESULTS

The To-336 strain of RV induces apoptosis of infected Vero cells

Vero cells infected with the To-336 strain of RV were analyzed for the hallmarks of apoptosis by different methods and compared to mock-infected cultures.

Indirect immunofluorescence assay to evaluate RV replication kinetics in infected Vero cells revealed positive staining for the RV E1 envelope glycoprotein on days 1, 3, 5, and 7 (Figs. 1B–D and 2D) in 10, 68, 98, and 98% of the cells, respectively. A similar, finely granular cytoplasmic staining pattern was observed using either polyclonal goat anti-rubella virus antiserum or rubella-positive human immune serum (data not shown). Thus, the Vero cell line is highly permissive to RV replication, consistent with previous studies (Hemphill *et al.,* 1988).

TdT-mediated digoxigenin–dUTP end-labeling (TUNEL) assay to determine whether the CPE of RV is due to apoptotic cell death revealed very few positive cells in mock-infected cultures (Figs. 2B and 2C), whereas 60–70% of cells in RV-infected cultures were positive, although some viable cells were still present even after the 7-day incubation (Figs. 2E and 2F). Thus, RV caused DNA damage characteristic of apoptosis in a substantial proportion of cells.

No cells treated with a UV-inactivated virus preparation were positive for expression of the RV E1 envelope glycoprotein by immunofluorescence assay (Fig. 2G) and no nuclei displayed positive TUNEL staining (Figs. 2H and 2I). The lack of detectable apoptosis in these cultures, together with the slow time course of the apoptotic response, suggests that productive virus infection is necessary to trigger cell death.

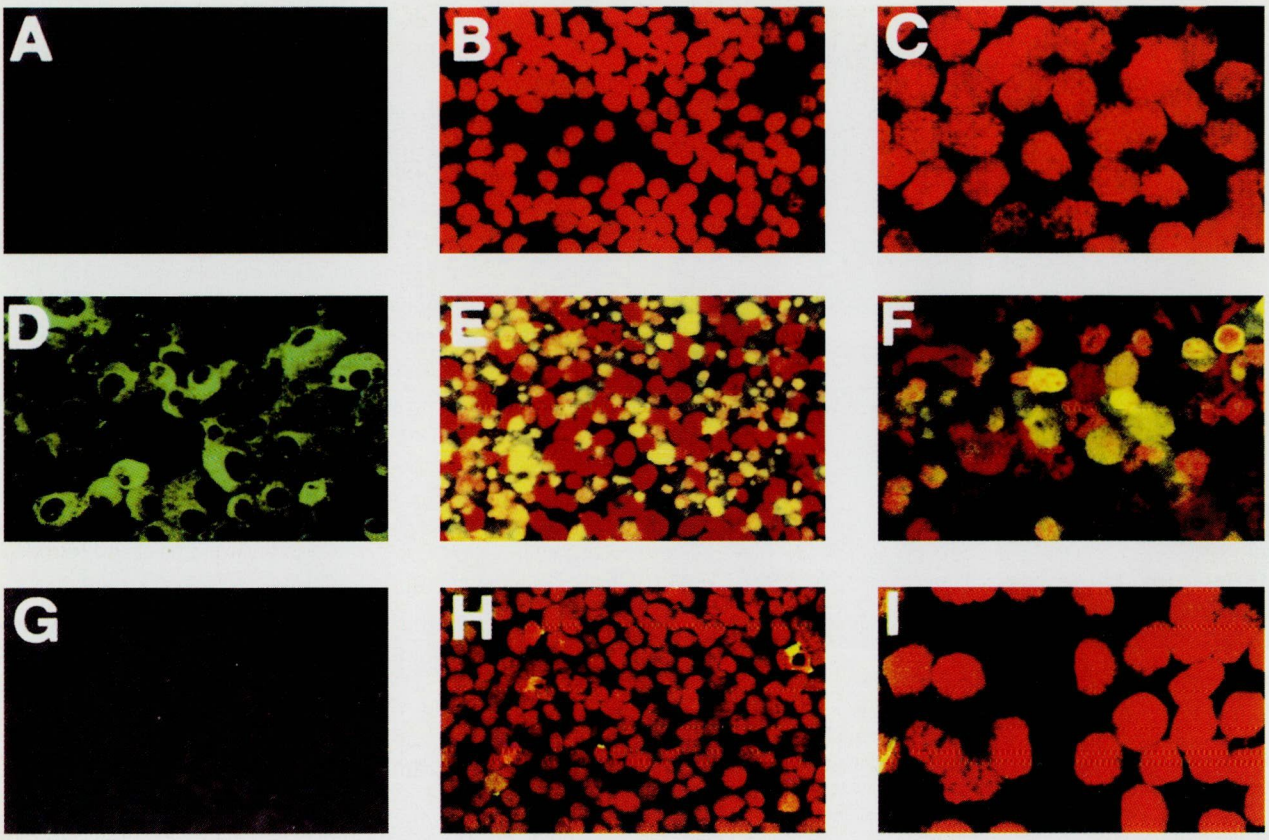

FIG. 2. Induction of apoptosis in Vero cells by RV. Vero cells infected with the To-336 strain of RV or treated with UV-irradiated virus were maintained for 7 days. Mock-infected cultures incubated in parallel were left untreated. RV replication was examined by indirect immunofluorescence assay (A, D, and G) as described in the Fig. 1 legend. (A) Mock-infected cells; (D and G) cells infected with RV or treated with UV-inactivated virus, respectively. *In situ* assay for apoptosis by the TUNEL method (B, C, E, F, H, and I): (B and C) mock-infected cultures; (E and F) cells infected with RV; (H and I) cells treated with UV-inactivated virus. All of the cultures were visualized by confocal microscopy and photographed at ×40 (B, E, and H) or ×100 (A, C, D, F, G, and I) magnification. Results are representative of three independent experiments.

Analysis of cellular DNA indicated DNA fragmentation from 3 days after virus inoculation, with the highest levels between 5 and 7 days postinfection (Fig. 3, lanes 6–8), whereas no DNA degradation was detected in the mock-infected cultures until 7 days of incubation, when a very weak DNA ladder appeared (Fig. 3, lanes 1–4). Thus, RV infection promotes the cleavage of cellular DNA into oligonucleosome-length fragments.

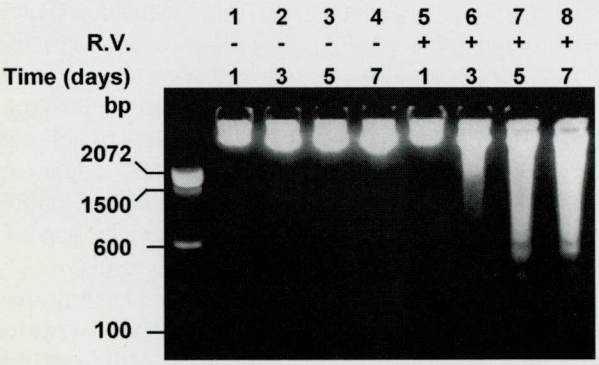

FIG. 3. Induction of apoptotic DNA fragmentation by RV infection in Vero cells. DNA was extracted from mock- or RV-infected cultures at the indicated time points, electrophoresed on a 1.8% agarose gel, and visualized by ethidium bromide staining. Lanes 1–4, mock-infected cultures; lanes 5–8, RV-infected cells. Results are representative of two independent experiments.

A double-parameter cytofluorometric DNA analysis to verify the presence of an apoptotic population in RV-infected cultures and to determine the distribution of proliferating cells within the different compartments of the cell cycle demonstrated that 1.5 and 46% of the total cell population in mock-infected and RV-infected cultures, respectively, had hypodiploid DNA content (Fig. 4). Moreover, the values calculated by the exclusion of apoptotic cells from the total number of cells indicated a decrease in active S phase (33%) and an accumulation in G2/M phase (18.5%) compared with mock-infected cells (41 and 10% in S phase and G2/M phase, respectively; Fig. 4). Thus, RV infection results in the appearance of cells with the hypodiploid DNA content characteristic of apoptosis and perturbs progression through the cell cycle.

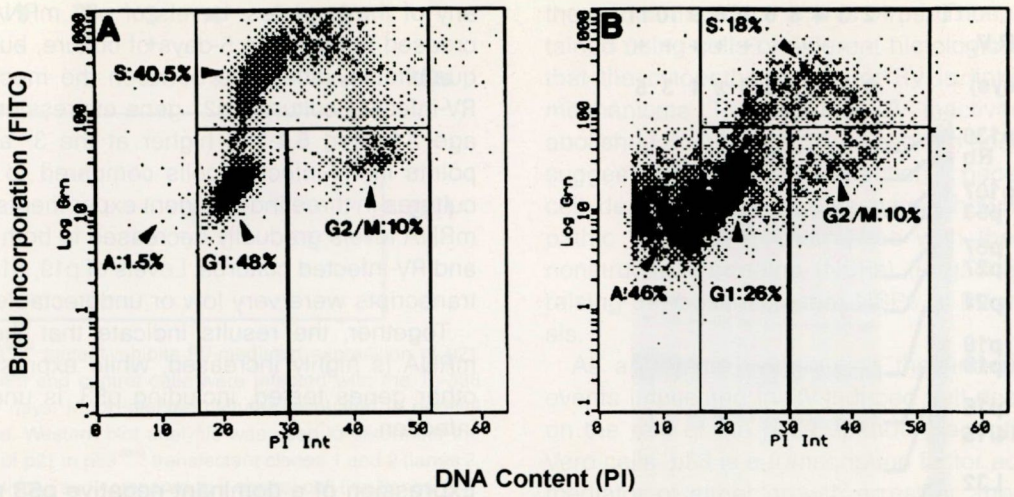

FIG. 4. Cell cycle distribution of RV-infected Vero cells. Asynchronously dividing mock (A)- and RV-infected (B) cells were analyzed simultaneously for DNA content with PI and for replicative DNA synthesis with FITC-conjugated anti-BrdU antibody, as described under Materials and Methods, using an EPICS XL flow cytometer. Results are representative of three independent experiments.

RV strain To-336 induces apoptosis in RK-13 cells but not in human embryonic fibroblast cell lines

To examine the ability of RV to induce apoptosis in other cell types, the extent of DNA fragmentation was measured in infected RK-13 cells and in two human embryonic fibroblast cell lines (HEL-17 and HEL-18) by ELISA. The results demonstrated that RV infection elicited apoptosis in RK-13 cells but not in fibroblast cell lines, compared with the corresponding mock-infected controls (Fig. 5). Indirect immunofluorescence assay to determine the frequency of infection revealed positive staining for the E1 antigen in 62% of RK-13 cells and in 54 and 58% of HEL-17 and HEL-18 fibroblasts, respectively. RV infection was accompanied by a visible CPE in RK-13 cells, but not in the fibroblast cell lines (data not shown). Thus, RV-induced apoptosis might be tissue-specific.

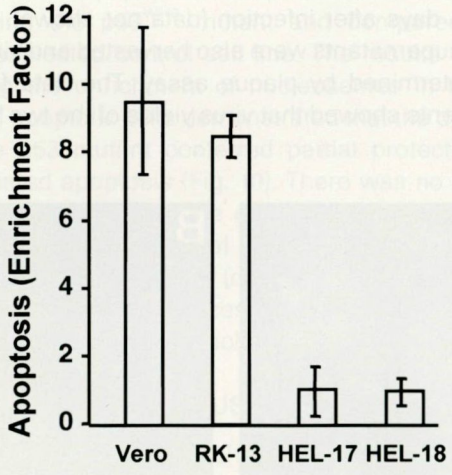

FIG. 5. Induction of apoptosis in RV-infected RK-13 cells, but not in human embryonic fibroblast cell lines. RV-induced apoptosis was measured by a specific ELISA in RK-13 cells and in two human embryonic fibroblast cell lines (HEL-17 and HEL-18) in comparison with the corresponding mock-infected controls at 7 days postinfection. Enrichment of the histone protein fraction associated with oligonucleosomal DNA in the cytoplasm of RV-infected cells was calculated as described under Materials and Methods. Data are mean (+SD) values from three independent experiments.

RV infection increases the levels of p53 and p21 proteins in Vero cells

To examine the potential role of p53 and p21 in the apoptotic response triggered by RV, the steady-state levels of these proteins were determined by Western blot analysis using the corresponding antibodies (Fig. 6). Endogenous p53 protein levels in the mock-infected cells were below the detection limit at the exposure shown in Fig. 6. However, low-level accumulation of p53 was detectable in these cultures by longer exposure of

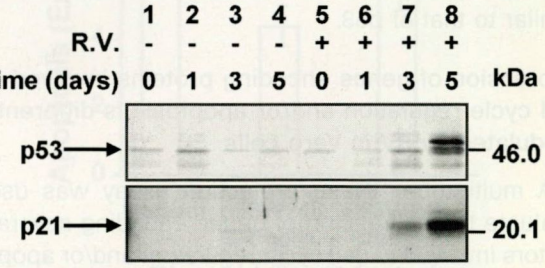

FIG. 6. RV infection increases the steady-state levels of p53 and p21 proteins in Vero cells. Total protein was isolated from mock-infected cells (lanes 1–5) and from RV-infected cells (lanes 6–10) at the indicated time points. Samples (50 mg of protein) were resolved on 12% SDS–PAGE and transferred to nitrocellulose filters. The steady-state levels of p53 and p21 proteins were analyzed by Western blot assay using the corresponding antibodies. Results are representative of three independent assays. The arrow for p53 refers to all three bands.

generated by limited proteolysis or may correspond to differentially phosphorylated isoforms of this protein. Expression of the p53 gene was unaffected by RV infection, suggesting that posttranscriptional regulatory mechanisms account for the increase in p53 protein levels. Comparison of the kinetics of p53 accumulation with the progression of apoptosis and CPE provided correlative evidence that RV-induced apoptosis might be mediated by p53. Expression of dominant-negative mutants is a method for determining the biological function of proteins (Malim *et al.*, 1989; Hassel *et al.*, 1993; Chen *et al.*, 1998; Ohnishi *et al.*, 1998). It has been shown that a single amino acid substitution, Trp248 (W248), which maps to the p53 DNA binding domain, confers dominant inhibitory activity to p53, because the mutant protein can oligomerize with wt p53 and abolish the sequence-specific DNA binding activity of the oligomer (Waterman *et al.*, 1996). To obtain further evidence for the importance of the p53-dependent pathway in cell death elicited by RV, we established Vero cell clones expressing dominant-negative p53 mutant ($p53^{W248}$). Our analysis revealed an impressive reduction of apoptosis in $p53^{W248}$ stable transfectants. On the other hand, this p53 mutant conferred only partial protection, since apoptosis was observed in clonal cell lines overexpressing $p53^{W248}$. It is possible that inhibition of endogenous p53 by $p53^{W248}$ was not complete or that multiple pathways of apoptosis are involved in the cellular response to RV infection. It is well-documented that p53 is rapidly stabilized following DNA damage (Nelson and Kastan, 1994), ribonucleotide depletion (Linke *et al.*, 1996), or hypoxia (Graeber *et al.*, 1994). Previous studies have also shown that p53 can be activated by binding of short single-stranded DNA fragments, as well as by interaction with cellular or viral proteins (Hupp *et al.*, 1995; Jayaraman and Prives, 1995; Waterman *et al.*, 1998). Recent observations emphasize the importance of phosphorylation events in the regulation of p53 activity (Martinez *et al.*, 1997; Shieh *et al.*, 1997; Waterman *et al.*, 1998). Although the detailed mechanisms of RV-mediated stabilization and activation of p53 remain to be elucidated, it is possible that RV leads to genotoxic stress, since genetic alterations, including chromosomal breakages, are known to occur following RV infection (Plotkin *et al.*, 1965b; Nusbacher *et al.*, 1967). Alternatively, virus replication may deplete cellular ribonucleotide pools and thereby contribute to the accumulation of p53.

RV infection also stimulated the expression of p21. Although G1 arrest mediated by p21 can inhibit p53-dependent apoptosis (Gorospe *et al.*, 1996, 1997), apoptosis can occur even in the presence of p21 (Polyak *et al.*, 1996; Sakamuro *et al.*, 1997). Cytofluorometric DNA analysis revealed no overt cell cycle block in the G1 phase due to RV infection, but instead the presence of a population with hypodiploid DNA content, demonstrating that apoptosis dominates over G1 arrest in a high proportion of cells. Recent data indicate that the biological consequence (i.e., G1 arrest or apoptosis) of the joint effect of p53 and p21 depends on their stoichiometric ratio as well as on the cellular context of their action determined by the histological type of cell and by the presence of extracellular signals (Chen *et al.*, 1996; Polyak *et al.*, 1996). Thus, while RV infection causes apoptosis in Vero cells, other cell types that are less susceptible to the cytopathogenic effect of the virus may show predominantly G1 arrest. This combination of CPE and mitotic inhibition is reflected in the pathology of CRS, which exhibits features of both destruction of specific tissues and growth retardation (Naeye and Blanc, 1965; Tondury and Smith, 1966; Driscoll, 1969; Plotkin, 1994). A possible role for p21 might be that of a mediator in the reconciliation of RV replication and cellular functions, promoting the noncytopathogenic form of infection and the establishment of viral persistence rather than mediating apoptosis.

Previous studies demonstrated that the simultaneous upregulation of bax and downregulation of bcl-2 synthesis increases the susceptibility of cells to apoptotic stimuli (Oltvai *et al.*, 1993). Our analysis revealed that the steady-state level of the p53-inducible bax-α protein is highly increased in RV-infected Vero cells (data not shown), which may contribute to cell destruction. Further studies that focus on the role of bcl-2 family member proteins appear promising in helping to establish the complex molecular mechanism of the teratogenic effect exerted by RV. Taken together, our data may bear on CRS, since tissue-specific apoptosis may account for certain dysfunctions observed in CRS patients.

MATERIALS AND METHODS

Cell culture and virus growth

Vero cells [obtained from the American Type Culture Collection (ATCC), Rockville, MD] were grown in Dulbecco's modified Eagle's minimal essential medium (Gibco/BRL, Grand Island, NY) supplemented with 7.5% fetal calf serum (Atlanta Biologicals, Norcross, GA). RK-13 cells (obtained from ATCC) were grown in Dulbecco's modified Eagle's medium (Gibco/BRL) supplemented with 10% fetal calf serum (Atlanta Biologicals). Human embryonic fibroblast cell lines HEL-17 and HEL-18 were maintained in RPMI medium (Sigma Chemical Co., St. Louis, MO) supplemented with 10% fetal calf serum (Gibco/BRL). All cell lines used were cultured at 35°C in a 5% CO_2 atmosphere.

To establish clonal cell lines expressing a dominant-negative p53 mutant ($p53^{W248}$), Vero cells were cotransfected with plasmid $pSVhp53^{W248}$, which directs expression of the mutant p53 protein, and plasmid pcDNA3 (Invitrogen, San Diego, CA), conferring G418 resistance (Waterman *et al.*, 1996). Cell lines cotransfected with pSV2 without insert and pcDNA3 served as mock-trans-

fected controls. Transfected cells were selected for G418 resistance, isolated, and expanded into cell lines. Expression of $p53^{W248}$ was examined by indirect immunofluorescence assay using MAb Ab-3 (clone PAb240; Calbiochem, Cambridge, MA), which detects only mutant p53, and Ab-5 (clone PAb1620; Calbiochem) MAb which detects only wild-type p53.

The To-336 strain of RV (obtained from ATCC, code VR-553) was propagated at a m. o. i. of 0.01 PFU per cell in Vero cell cultures for 7 days at 35°C. The culture fluid of RV-infected Vero cells was harvested, stored at −70°C, and used as infecting stock of virus.

Virus plaque assay was performed as described (Sato *et al.,* 1979) on confluent monolayers of Vero cells inoculated with virus solution for 1 h at 35°C and overlaid with 0.5% agarose (FMC, Rockland, ME) in phenol red-free Eagle's minimum essential medium supplemented with 7.5% fetal bovine serum and 2 mM L-glutamine. After 4 days of culture at 35°C, a second agarose overlay containing 0.005% neutral red was added. Plaque titers were determined at 7 days after virus infection.

Unless otherwise indicated, Vero cell cultures were infected with the To-336 strain of RV at a m. o. i. of 5 PFU per cell. For experiments using inactivated virus, culture fluid containing 1×10^7 PFU/ml RV virions was exposed to UV light (254 nm) for 20 min at a distance of 10 cm. Lack of infectious virus (<5 PFU/ml) in UV-irradiated virus stock was verified by plaque assay.

Indirect immunofluorescence assay

Cytospin (Shandon Inc., Pittsburgh, PA) cell preparations were fixed in methanol–acetone (1:1) for 15 min at −20°C. Slides were incubated with a 1:100 dilution of RV glycoprotein E1-specific MAb (Biodesign, Kennebunk, ME) for 1 h at 37°C. Alternatively, a polyclonal goat anti-RV immunoglobulin (1:200) (Biodesign) or a rubella-positive human immune serum (1:30) was used as primary antibody in some experiments. After washing with PBS, samples were reacted with fluorescein isothiocyanate (FITC)-conjugated species-specific secondary antibodies [1:800 dilution of FITC-labeled anti-mouse antibody (Cappel, Durham, NC), or FITC-labeled anti-goat antibody (1:100) (PharMingen, San Diego, CA), or FITC-labeled anti-human antibody (1:100) (Sigma Chemical Co.)] and incubated for 1 h at 37°C. After washing with PBS, slides were counterstained with 0.01% Evans blue (Sigma) and visualized by confocal microscopy. The ratio of positive to negative cells was determined after counting 1000 cells in random fields.

DNA fragmentation analysis

Cells (2×10^6) were resuspended in lysis buffer containing 50 mM Tris–HCl, pH 8.0, 10 mM NaCl, 10 mM EDTA, 0.5% *N*-lauroyl sarcosine, 100 mg/ml proteinase K (Boehringer-Mannheim, Indianapolis, IN) and incubated for 2 h at 37°C. Lysed cells were subjected to phenol–chloroform extraction. Nucleic acids were precipitated with 0.1 M NaCl and 2.5 vol of ice-cold absolute ethanol. Following centrifugation at 12,000 rpm at 4°C, pellets were resuspended in RNase buffer consisting of 15 mM NaCl, 10 mM Tris–HCl, pH 7.5, and 50 mg/ml RNaseA (Sigma). Incubation was carried out for 1 h at 37°C. DNA was reextracted with phenol–chloroform, precipitated, and resuspended in 10 mM Tris–HCl, pH 7.5, 1 mM EDTA. DNA samples (20 mg each) were electrophoretically separated on 1.8% agarose gel containing ethidium bromide and visualized under UV light.

TUNEL assay for DNA degradation

In situ assay for apoptosis was performed by direct immunofluorescence detection of digoxigenin-labeled DNA. Cytospin cell preparations were fixed in 1% paraformaldehyde for 30 min at room temperature. Samples were treated with 20 mg/ml proteinase K (Boehringer-Mannheim) for 15 min at room temperature. Terminal deoxynucleotidyl transferase (TdT; Oncor Inc., Gaithersburg, MD) was applied to incorporate digoxigenin-11-dUTP at sites of DNA breaks for 1 h at 37°C. Incubation with FITC-conjugated anti-digoxigenin antibody (Oncor Inc.) was carried out for 30 min at room temperature. Negative control sections were treated identically except for the omission of the TdT enzyme. After the TUNEL assay, cytospin preparations were also stained in PBS containing 1 mg/ml propidium iodide (PI) (Sigma) and 50 mg/ml RNaseA (Sigma) for 15 min at 37°C. Nuclear fluorescence of stained cells was visualized by confocal microscopy. Apoptotic cells labeled with FITC display yellow fluorescence, while viable cells stained only by PI appear as red nuclei.

Quantitation of apoptosis by ELISA

Cells were washed in PBS and the cell pellet was processed in a cell death detection ELISA kit that is based on the detection of core histones (H2A, H2B, H3, and H4) complexed with mono- and oligonucleosome fragments formed during cell death, using anti-histone MAb. This system allows the specific detection of histone proteins in the cytoplasmic fraction (Boehringer-Mannheim). Cells were incubated in lysis buffer for 30 min at 4°C and centrifuged at 12,000 rpm for 10 min, and supernatants were tested by ELISA. Microtiter plates were coated with anti-histone MAb for 1 h at room temperature. Each sample was incubated in duplicate for 90 min at room temperature, washed, and incubated with peroxidase-conjugated antibody (anti-DNA-POD) for 90 min at room temperature. After washing, substrate solution (ABTS) was added to each well for 5–10 min. Absorbance was measured at 405 and 620 nm. Specific enrichment of mono- and oligonucleosomes released into the cytoplasm was calculated as: absorbance of RV-

infected cells/absorbance of corresponding mock-infected control cells = enrichment factor.

Cytofluorometric DNA analysis

At 2 days postinfection, cells were trypsinized and subcultivated at approximately 30% confluency for 2 more days to obtain an asynchronously dividing cell population. Mock-infected cultures were cultured in parallel. Cells were pulse-labeled for 50 min with 10 mM bromodeoxyuridine (BrdU) (Sigma), trypsinized, washed with PBS, and fixed in 70% ethanol for 30 min at room temperature. After washing with PBS containing 0.5% BSA, cells were resuspended in denaturing solution (2 M HCl and 0.5% Triton X-100) and incubated for 20 min at room temperature. After another PBS wash, cell pellets were resuspended in 0.1 M sodium borate ($Na_2B_4O_7$), pH 8.5, to neutralize any residual acid, incubated with anti-BrdU MAb (PharMingen) for 1 h at room temperature, washed with PBS containing 0.5% BSA, and further incubated with FITC-conjugated anti-mouse IgG (PharMingen) for 30 min at room temperature. Cells were then treated with RNaseA, stained with 1 mg/ml PI for 20 min at room temperature, and analyzed using an EPICS XL flow cytometer (Coulter Corp., Hialeah, FL).

Western blot assay

Cells ($5–10 \times 10^6$) were lysed in buffer containing 150 mM NaCl, 10 mM Tris–HCl, pH 7.6, 5 mM EDTA, 1% (v/v) Nonidet P-40, 0.1% SDS, 1% sodium deoxycholate, 2 mM phenylmethylsulfonyl fluoride, 50 mg/ml aprotinin, 50 mg/ml leupeptin, and 20 mM NaF for 30 min at 4°C, sheared through a fine-gauge needle until no longer viscous, and centrifugated for 10 min at 10,000 *g* to remove cell debris and nuclei. Protein concentration of cell lysates was determined using the Bio-Rad protein assay (Bio-Rad, Hercules, CA). Supernatants were mixed with Laemmli's sample buffer and boiled for 3 min. Aliquots (50 mg) of total protein were resolved by SDS–PAGE and electrotransferred onto nitrocellulose filters (Amersham, Buckinghamshire, UK). Preblocked blots were reacted with specific antibodies to p53 (clone DO-1; Oncogene Science Inc., Cambridge, MA), p21 (Santa Cruz Biotechnology, Inc., Santa Cruz, CA), and bax (PharMingen) in PBS containing 0.05% (v/v) Tween 20, 1% (w/v) dried nonfat milk (Difco Laboratories, Detroit, MI), and 1% (w/v) BSA (fraction V; Sigma). Blots were then incubated for 2 h with species-specific secondary antibodies coupled to peroxidase (Amersham). Filters were washed in PBS–Tween five times for 5 min between each step and were developed using a chemiluminescent detection system (Amersham).

RNase protection assay

Total RNA was isolated using the TRIZOL reagent (Gibco/BRL) according to the manufacturer's protocol. Expression of various genes involved in cell cycle regulation and apoptosis was analyzed by RNase protection assay using the RiboQuant RPA System kit, as outlined by the supplier (PharMingen). Briefly, anti-sense RNA probe sets were transcribed by T7 polymerase and radiolabeled with [α-^{32}P]UTP (3000 Ci/mmol, DuPont NEN, Boston, MA). The hCC-2 multiprobe template set (catalog No. 45091P) allows the simultaneous detection of mRNAs encoding p130, Rb, p107, p53, p57, p27, p21, p19, p18, p16, p14/15, L32, and GAPDH. RNA samples (10 mg each) were mixed with the hCC-2 riboprobe set (8×10^5 cpm/sample), heated to 90°C, and incubated at 56°C for 12 h. Single-stranded RNA was digested by the addition of RNaseA and RNaseT1. After treatment with proteinase K, the remaining RNA duplexes were purified by phenol/chloroform extraction, precipitated, and redissolved. Size fractionation of the protected probes was carried out by electrophoresis on 5%/8 M urea sequencing gels. Dried gels were exposed to Kodak X-ray films (Kodak, Rochester, NY) and visualized by autoradiography. Simultaneous detection of housekeeping gene transcription (L32) as an internal control was used for the quantitative evaluation of the data by phosphorimaging.

ACKNOWLEDGMENTS

We thank Bela Tarodi for stimulating discussions, Quinwu Lin for assistance with confocal microscopy, and Jeffrey S. Faust for assistance with cytofluorometric DNA analysis. We also thank the Editorial Department of the Wistar Institute for preparing the manuscript. This work was supported by the Taxin Memorial Fund and the OTKA T 026040.

Note added in proof. While this work was in progress K. V. Pugachev and T. K. Frey (*Virology* **250**, 359–370, 1998) reported that the Therien strain of RV induces apoptosis in Vero cells.

REFERENCES

Allday, M. J., Sinclair, A., Parker, G., Crawford, D. H., and Farrell, P. J. (1995). Epstein-Barr virus efficiently immortalizes human B cells without neutralizing the function of p53. *EMBO J.* **14**, 1382–1391.

Bellanti, J. A., Artenstein, M. S., Olson, L. C., Buescher, E. L., Luhrs, C. E., and Milstead, K. L. (1965). Congenital rubella: Clinicopathologic, virologic and immunologic studies. *Am. J. Dis. Child.* **110**, 464–472.

Bowden, D. S., Pedersen, J. S., Toh, B. H., and Westaway, E. G. (1987). Distribution by immunofluorescence of viral products and actin-containing cytoskeletal filaments in rubella virus-infected cells. *Arch. Virol.* **92**, 211–219.

Caelles, C., Helmberg, A., and Karin, M. (1994). p53-dependent apoptosis in the absence of transcriptional activation of p53-target genes. *Nature* **370**, 220–223.

Chen, W., and Cooper, N. R. (1996). Epstein-Barr virus nuclear antigen 2 and latent membrane protein independently transactivate p53 through induction of NF-kB activity. *J. Virol.* **70**, 4849–4853.

Chen, W., Huang, S., and Cooper, N. R. (1998). Levels of p53 in Epstein-Barr virus-infected cells determine cell fate: Apoptosis, cell cycle arrest at the G1/S boundary without apoptosis, cell cycle arrest at the G2/M boundary without apoptosis, or unrestricted proliferation. *Virology* **251**, 217–226.

Chen, X., Ko, L. J., Jayaraman, L., and Prives, C. (1996). p53 levels,

functional domains, and DNA damage determine the extent of the apoptotic response of tumor cells. *Genes Dev.* **10**, 2438–2451.

Chirillo, P., Pagano, S., Natoli, G., Puri, P. L., Burgio, V. L., Balsano, C., and Levrero, M. (1997). The hepatitis B virus X gene induces p53-mediated programmed cell death. *Proc. Natl. Acad. Sci. USA* **94**, 8162–8167.

Debbas, M., and White, E. (1993). Wild-type p53 mediates apoptosis by E1A, which is inhibited by E1B. *Genes Dev.* **7**, 546–554.

Desaintes, C., Demeret, C., Goyat, S., Yaniv, M., and Thierry, F. (1997). Expression of the papillomavirus E2 protein in HeLa cells leads to apoptosis. *EMBO J.* **16**, 504–514.

Diaz-Guerra, M., Rivas, C., and Esteban, M. (1997). Activation of the IFN-inducible enzyme RNase L causes apoptosis of animal cells. *Virology* **236**, 354–363.

Driscoll, S. G. (1969). Histopathology of gestational rubella. *Am. J. Dis. Child.* **118**, 49–53.

Dudgeon, J. A. (1969). Congenital rubella: Pathogenesis and immunology. *Am. J. Dis. Child.* **118**, 35–44.

El-Deiry, W. S., Tokino, T., Velculescu, V. E., Levy, D. B., Parsons, R., Trent, J. M., Lin, D., Mercer, W. E., Kinzler, K. W., and Vogelstein, B. (1993). WAF1, a potential mediator of p53 tumor suppression. *Cell* **75**, 817–825.

Gillet, G., and Brun, G. (1996). Viral inhibition of apoptosis. *Trends Microbiol.* **4**, 312–317.

Gorospe, M., Cirielli, C., Wang, X., Seth, P., Capogrossi, M. C., and Holbrook, N. J. (1997). $p21^{WAF1/CIP1}$ protects against p53-mediated apoptosis of human melanoma cells. *Oncogene* **14**, 929–935.

Gorospe, M., Wang, X., Guyton, K. Z., and Holbrook, N. J. (1996). Protective role of $p21^{WAF1/CIP1}$ against prostaglandin A_2-mediated apoptosis of human colorectal carcinoma cells. *Mol. Cell. Biol.* **16**, 6654–6660.

Gottlieb, M. T., and Oren, M. (1996). p53 in growth control and neoplasia. *Biochem. Biophys. Acta* **1287**, 77–102.

Graeber, T. G., Peterson, J. F., Tsai, M., Monica, K., Fornace, A. J. Jr., and Giaccia, A. J. (1994). Hypoxia induces accumulation of p53 protein, but activation of a G_1-phase checkpoint by low-oxygen conditions is independent of p53 status. *Mol. Cell. Biol.* **14**, 6264–6277.

Griffin, D. E., and Hardwick, J. M. (1997). Regulators of apoptosis on the road to persistent alphavirus infection. *Annu. Rev. Microbiol.* **51**, 565–592.

Hassel, B. A., Zhou, A., Sotomayor, C., Maran, A., and Silverman, R. H. (1993). A dominant negative mutant of 2-5A-dependent RNAse suppresses antiproliferative and antiviral effects of interferon. *EMBO J.* **12**, 3297–3304.

Haupt, Y., Rowan, S., Shaulian, E., Voudsen, K., and Oren, M. (1995). Induction of apoptosis in HeLa cells by transactivation-deficient p53. *Genes Dev.* **9**, 2170–2183.

Hemphill, M. L., Forng, R.-Y., Abernathy, E. S., and Frey, T. K. (1988). Time course of virus-specific macromolecular synthesis during rubella virus infection in Vero cells. *Virology* **162**, 65–75.

Hupp, T. R., Sparks, A., and Lane, D. P. (1995). Small peptides activate the latent sequence-specific DNA binding function of p53. *Cell* **83**, 237–245.

Jansen-Dürr, P. (1996). How viral oncogenes make the cell cycle. *Trends Genet.* **12**, 270–276.

Jayaraman, L., and Prives, C. (1995). Activation of p53 sequence-specific DNA binding by short single strands of DNA requires the p53 C-terminus. *Cell* **81**, 1021–1029.

Joe, A. K., Foo, H. H., Kleeman, L., and Levine, B. (1998). The transmembrane domains of Sindbis virus envelope glycoproteins induce cell death. *J. Virol.* **72**, 3935–3943.

Ko, L. J., and Prives, C. (1996). p53: Puzzle and paradigm. *Genes Dev.* **10**, 1054–1072.

Lee, J. Y., Bowden, D. S., and Marshall, J. A. (1996). Membrane junctions associated with rubella virus infected cells. *J. Submicrosc. Cytol. Pathol.* **28**, 101–108.

Lee, S. B., Rodriquez, D., Rodriquez, J. R., and Esteban, M. (1997). The apoptosis pathway triggered by the interferon-induced protein kinase PKR requires the third basic domain, initiates upstream of Bcl-2, and involves ICE-like proteases. *Virology* **231**, 81–88.

Levine, B., Huang, Q., Isaacs, J. T., Reed, J. C., Griffin, D. E., and Hardwick, J. M. (1993). Conversion of lytic to persistent alphavirus infection by the bcl-2 cellular oncogene. *Nature* **361**, 739–742.

Levine, B., Goldman, J. E., Jiang, H. H., Griffin, D. E., and Hardwick, J. M. (1996). Bcl-2 protects mice against fatal alphavirus encephalitis. *Proc. Natl. Acad. Sci. USA* **93**, 4810–4815.

Lewis, J., Wesselingh, S. L., Griffin, D. E., and Hardwick, J. M. (1996). Alphavirus-induced apoptosis in mouse brains correlates with neurovirulence. *J. Virol.* **70**, 1828–1835.

Lin, K.-I., Lee, S.-H., Narayanan, R., Baraban, J. M., Hardwick, J. M., and Ratan, R. R. (1995). Thiol agents and bcl-2 identify an alphavirus-induced apoptotic pathway that requires activation of the transcription factor NF-kappa B. *J. Cell Biol.* **131**, 1149–1161.

Lin, K.-I., DiDonato, J. A., Hoffman, A., Hardwick, J. M., and Ratan, R. R. (1998). Suppression of steady-state, but not stimulus-induced NF-kappa B activity inhibits alphavirus-induced apoptosis. *J. Cell Biol.* **141**, 1479–1487.

Linke, S. P., Clarkin, K. C., Di Leonardo, A., Tsou, A., and Wahl, G. M. (1996). A reversible, p53-dependent G_0/G_1 cell cycle arrest induced by ribonucleotide depletion in the absence of detectable DNA damage. *Genes Dev.* **10**, 934–947.

Lowe, S. W., and Ruley, H. E. (1993). Stabilization of the p53 tumor suppressor is induced by adenovirus 5 E1A and accompanies apoptosis. *Genes Dev.* **7**, 535–545.

Malim, M. H., Bohnlein, S., Hauber, J., and Cullen, B. R. (1989). Functional dissection of the HIV-1 Rev trans-activator-derivation of a trans-dominant repressor of Rev function. *Cell* **58**, 205–214.

Martinez, J. D., Craven, M. T., Joseloff, E., Milczarek, G., and Bowden, G. T. (1997). Regulation of DNA binding and transactivation in p53 by nuclear localization and phosphorylation. *Oncogene* **14**, 2511–2520.

McCarthy, K. (1969). Cell cultures useful for the study of rubella. *Am. J. Dis. Child.* **118**, 78–83.

Miyashita, T., and Reed, J. C. (1995). Tumor suppressor p53 is a direct transcriptional activator of the human bax gene. *Cell* **80**, 293–299.

Naeye, R. L., and Blanc, W. (1965). Pathogenesis of congenital rubella. *J. Am. Med. Assoc.* **194**, 1277–1283.

Nelson, W. G., and Kastan, M. B. (1994). DNA strand breaks: The DNA template alterations that trigger p53-dependent DNA damage response pathways. *Mol. Cell. Biol.* **14**, 1815–1823.

Nusbacher, J., Hirschhorn, K., and Cooper, L. Z. (1967). Chromosomal abnormalities in congenital rubella. *N. Eng. J. Med.* **276**, 1409–1413.

Okan, I., Wang, Y., Chen, F., Hu, L. F., Imreh, S., Klein, G., and Wiman, K. G. (1995). The EBV-encoded LMP1 protein inhibits p53-triggered apoptosis but not growth arrest. *Oncogene* **11**, 1027–1031.

Oltvai, Z. N., Milliman, C. L., and Korsmeyer, S. J. (1993). Bcl-2 heterodimerizes in vivo with a conserved homolog, Bax, that accelerates programmed cell death. *Cell* **74**, 609–619.

Ohnishi, T., Wang, X., Ohnishi, K., and Takahashi, A. (1998). p53-dependent induction of WAF1 by cold shock in human glioblastoma cells. *Oncogene* **16**, 1507–1511.

Plotkin, S. A. (1994). Rubella vaccine. *In* "Vaccines," 2nd ed. (S. A. Plotkin and E. A. Mortimer, Eds.), pp. 303–336. Saunders, Philadelphia.

Plotkin, S. A., Oski, F. A., Hartnett, E. M., Hervada, A. R., Friedman, S., and Gowing, F. (1965a). Some recently recognized manifestations of the rubella syndrome. *J. Pediatr.* **67**, 182–191.

Plotkin, S. A., Boue, A., and Boue, J. G. (1965b). The in vitro growth of rubella virus in human embryo cells. *Am. J. Epidemiol.* **81**, 71–85.

Plotkin, S. A., and Vaheri, A. (1967). Human fibroblasts infected with rubella virus produce a growth inhibitor. *Science* **156**, 659–661.

Polyak, K., Waldman, T., He, T.-C., Kinzler, K. W., and Vogelstein, B. (1996). Genetic determinants of p53-induced apoptosis and growth arrest. *Genes Dev.* **10**, 1945–1952.

Pugachev, K. V., Abernathy, E. S., and Frey, T. K. (1997). Improvement of the specific infectivity of the rubella virus (RUB) infectious clone:

Determinants of cytopathogenicity induced by RUB map to the nonstructural proteins. *J. Virol.* **71**, 562–568.

Pugachev, K. V., and Frey, T. K. (1998). Rubella virus induces apoptosis in culture cells. *Virology* **250**, 359–370.

Rawls, W. E., and Melnick, J. L. (1966). Rubella virus carrier cultures derived from congenitally infected infants. *J. Exp. Med.* **123**, 795–816.

Razvi, E. S., and Welsh, R. M. (1995). Apoptosis in viral infections. *Adv. Virus Res.* **45**, 1–60.

Sabbatini, P., Lin, J., Levine, A. J., and White, E. (1995). Essential role for p53-mediated transcription in E1A-induced apoptosis. *Genes Dev.* **9**, 2184–2192.

Sakamuro, F., Sabbatini, P., White, E., and Prendergast, G. C. (1997). The polyproline region of p53 is required to activate apoptosis but not growth arrest. *Oncogene* **15**, 887–898.

Sato, H., Albrecht, P., and Ennis, F. A. (1979). A novel plaque method for attenuated rubella virus in Vero cell cultures. *Arch. Virol.* **59**, 281–284.

Shieh, S. Y., Ikeda, M., Taya, Y., and Prives, C. (1997). DNA damage-induced phosphorylation of p53 alleviates inhibition by Mdm2. *Cell* **91**, 325–334.

Singer, D. B., Rudolph, A. J., Rosenberg, H. S., Rawls, W. E., and Boniuk, M. (1967). Pathology of the congenital rubella syndrome. *Pediatrics* **71**, 665–675.

Strack, P. R., Frey, M. W., Rizzo, C. J., Cordova, B., George, H. J., Meade, R., Ho, S. P., Corman, J., Tritch, R., and Korant, B. D. (1996). Apoptosis mediated by HIV protease is preceded by cleavage of Bcl-2. *Proc. Natl. Acad. Sci. USA* **93**, 9571–9576.

Su, F., and Schneider, R. J. (1997). Hepatitis B virus HBx protein sensitizes cells to apoptotic killing by tumor necrosis factor α. *Proc. Natl. Acad. Sci. USA* **94**, 8744–8749.

Subramanian, T., Tarodi, B., and Chinnadurai, G. (1995). p53-independent apoptotic and necrotic cell deaths induced by adenovirus infection: Suppression by E1B 19K and Bcl-2 proteins. *Cell Growth Differ.* **6**, 131–137.

Subramanian, T., Tarodi, B., Govindarajan, R., Boyd, J. M., Yoshida, K., and Chinnadurai, G. (1993). Mutational analysis of the transforming and apoptosis suppression activities of the adenovirus E1B 175R protein. *Gene* **124**, 173–181.

Takizawa, T., Ohashi, K., and Nakanishi, Y. (1996). Possible involvement of double-stranded RNA-activated protein kinase in cell death by influenza virus infection. *J. Virol.* **70**, 8128–8132.

Tondury, G., and Smith, D. W. (1966). Fetal rubella pathology. *J. Pediatr.* **68**, 867–879.

Xiong, Y., Hannon, G., Zhang, H., Casso, D., Kobayashi, R., and Beach, D. (1993). p21 is a universal inhibitor of cyclin kinases. *Nature* **366**, 701–704.

Wada, N., Matsumura, M., Ohba, Y., Kobayashi, N., Takizawa, T., and Nakanishi, Y. (1995). Transcription stimulation of the Fas-encoding gene by nuclear factor for interleukin-6 expression upon influenza virus infection. *J. Biol. Chem.* **270**, 18007–18012.

Waterman, M. J. F., Waterman, J. L. F., and Halazonetis, T. D. (1996). An engineered four-stranded coiled coil substitutes for the tetramerization domain of wild-type p53 and alleviates transdominant inhibition by tumor-derived p53 mutants. *Cancer Res.* **56**, 158–163.

Waterman, M. J. F., Stavridi, E. S., Waterman, J. L. F., and Halazonetis, T. D. (1998). ATM-dependent activation of p53 involves dephosphorylation and association with 14-3-3 proteins. *Nature Genet.* **19**, 175–178.

Wolinsky, J. S. (1996). Rubella. *In* "Fields Virology," 3rd ed. (B. N. Fields, D. M. Knipe, P. M. Howley *et al.*, Eds.), pp. 899–929. Lippincott–Raven, Philadelphia.

Yoneda, T., Urade, M., Sakuda, M., and Miyazaki, T. (1986). Altered growth, differentiation, and responsiveness of epidermal growth factor of human embryonic mesenchymal cells of palate by persistent rubella virus infection. *J. Clin. Invest.* **77**, 1613–1621.